Pulmonary immune response regulation, genotoxicity, and metabolic reprogramming by menthol- and tobacco-flavored e-cigarette exposures in mice

Thivanka Muthumalage, Irfan Rahman [ID]*

Department of Environmental Medicine, School of Medicine and Dentistry, University of Rochester Medical Center, Rochester, New York 14642, USA

*To whom address should be addressed at Department of Environmental Medicine, School of Medicine and Dentistry, University of Rochester Medical Center, Box 850, 601 Elmwood Avenue, Rochester, NY 14642, USA. E-mail: irfan_rahman@urmc.rochester.edu.
Disclaimer: The authors have nothing to claim or disclaim about any products used here to test their toxicological and biological effects. The authors have no personal interests or gains from the outcome of this study. No commercial interests with e-liquid manufacturers.

Abstract

Menthol and tobacco flavors are available for almost all tobacco products, including electronic cigarettes (e-cigs). These flavors are a mixture of chemicals with overlapping constituents. There are no comparative toxicity studies of these flavors produced by different manufacturers. We hypothesized that acute exposure to menthol and tobacco-flavored e-cig aerosols induces inflammatory, genotoxicity, and metabolic responses in mouse lungs. We compared two brands, A and B, of e-cig flavors (PG/VG, menthol, and tobacco) with and without nicotine for their inflammatory response, genotoxic markers, and altered genes and proteins in the context of metabolism by exposing mouse strains, C57BL/6J (Th1-mediated) and BALB/cJ (Th2-mediated). Brand A nicotine-free menthol exposure caused increased neutrophils and differential T-lymphocyte influx in bronchoalveolar lavage fluid and induced significant immunosuppression, while brand A tobacco with nicotine elicited an allergic inflammatory response with increased Eotaxin, IL-6, and RANTES levels. Brand B elicited a similar inflammatory response in menthol flavor exposure. Upon e-cig exposure, genotoxicity markers significantly increased in lung tissue. These inflammatory and genotoxicity responses were associated with altered NLRP3 inflammasome and TRPA1 induction by menthol flavor. Nicotine decreased surfactant protein D and increased PAI-1 by menthol and tobacco flavors, respectively. Integration of inflammatory and metabolic pathway gene expression analysis showed immunometabolic regulation in T cells via PI3K/Akt/p70S6k-mTOR axis associated with suppressed immunity/allergic immune response. Overall, this study showed the comparative toxicity of flavored e-cig aerosols, unraveling potential signaling pathways of nicotine and flavor-mediated pulmonary toxicological responses, and emphasized the need for standardized toxicity testing for appropriate premarket authorization of e-cigarette products.

Keywords: e-cigarettes; ENDS; flavors; menthol; tobacco; nicotine; immunometabolism; hypersensitivity

Electronic nicotine delivery systems (ENDS) or electronic cigarettes (e-cigs) have become popular as a cessation method, with declined use of combustible cigarettes. However, the use of ENDS by nonsmokers is on the rise, especially among youth (Galderisi *et al.*, 2020; Levy *et al.*, 2019). Contradictory to the intended use of ENDS as a cessation tool, flavored ENDS has become a gateway to nicotine use and nicotine/vaping addiction, as more than 20% of high schoolers and middle-schoolers were using e-cigs in 2021 (Hamberger and Halpern-Felsher, 2020; Miech *et al.*, 2021). Despite all efforts by regulatory agencies, a plethora of nicotine-containing ENDS (vape bars, e-liquids, pods) is available in retail stores and online. Similarly, menthol-, mint-, cooling-, and tobacco-flavored ENDS are available in many forms, such as e-liquids, disposable vapes, and pod-based products. However, with increased regulation policies by the Food and Drug Administration, such as the flavor ban and premarket authorization, menthol- and tobacco-flavored ENDS sales and consumption has been rising, while other flavored ENDS sales have been declining (Ali *et al.*, 2022; Diaz *et al.*, 2021).

E-liquids contain humectants, flavoring chemicals, and additives, such as flavor enhancers forming secondary pyrolytic products upon heating. These degradation products depend on many factors, such as the temperature of the coil and the power (wattage) of the device (Bitzer *et al.*, 2018; Li *et al.*, 2021b). We have shown that certain flavoring chemicals cause more toxicity and inflammation than others (Kaur *et al.*, 2018; Lamb *et al.*, 2020, 2022; Muthumalage *et al.*, 2017, 2019). We and others have shown that secondary degradation products, such as aldehydes in menthol, tobacco, cinnamon, and fruit-flavored e-liquids, cause mitochondrial dysfunction, cellular toxicity, inflammation, and impaired phagocytosis (Hickman *et al.*, 2019; Hua *et al.*, 2019; Jabba *et al.*, 2020; Khlystov and Samburova, 2016; Omaiye *et al.*, 2019). Subacute to subchronic exposure to flavored ENDS has shown moderate levels of lung inflammation and immune response in mice (Crotty Alexander *et al.*, 2018; Szafran *et al.*, 2020). In our previous studies, we have shown that flavoring chemicals generate reactive oxygen species, causing epithelial barrier dysfunction, oxidative stress, cytotoxicity, inflammation,

mitochondrial dysfunction, DNA damage, and cellular senescence *in vitro* and *in vivo* in mouse lungs (Lamb *et al.*, 2020, 2022; Lei *et al.*, 2017; Lerner *et al.*, 2015; Lucas *et al.*, 2020; Muthumalage *et al.*, 2019; Wang *et al.*, 2020). E-cigarette, or Vaping-Induced lung Injury epidemic was primarily associated with e-cigarettes using THC-containing cartridges, but we have found the presence of nicotine and flavors in those cartridges (Muthumalage *et al.*, 2020). While researchers have identified individual cellular processes, the exact mechanism of vaping-induced lung injury is unclear (Alexander *et al.*, 2020).

Currently, no standardized manufacturing guidelines are practiced during e-cigarette flavor production for chemical ingredients, such as PG/VG, nicotine, and flavoring agents. Different manufacturers/vendors produce the same e-cig flavor using various proportions of humectants, flavoring agents, and nicotine and label them as a particular flavor, eg, tobacco and menthol. While we have observed acute lung injury and priming of pathogenic processes, such as extracellular matrix remodeling due to PG/VG and nicotine exposure, flavor interaction-induced lung damage has not yet been studied. Furthermore, comparative toxicity assessment of the same flavor by two brands has not been investigated. E-cigs of the same flavor by different vendors may have differential toxicity. Hence, we assessed two locally purchased e-liquid brands of PG/VG, menthol, and tobacco flavors with and without nicotine, using two strains of mice (C57BL/6J and BALB/cJ, both male and female). These variables were selected to minimize bias and generalization by using just one brand of e-liquid. In this study, we performed a comparative toxicological analysis, focusing on inflammation, genotoxicity, and cellular metabolism to shed light on acute phase lung injury and resolution.

As the chemosensory cation channel receptors have been observed to play a role in cough reflex sensitivity in lung diseases such as asthma, chronic obstructive pulmonary disease (COPD), and idiopathic pulmonary fibrosis (IPF), we assessed transient receptor potential ankyrin 1 (TRPA1) expression in lung homogenates. Flavoring chemicals in e-cig aerosols have not been well studied as an agonist of TRPA1, though expressed in bronchial epithelial cells and lung fibroblasts and have been associated with allergic asthma (Caceres *et al.*, 2009). The pivotal roles of these intracellular immune receptors/sensors, and inflammasomes, in sensing systemic metabolic perturbations have recently become evident. We have shown augmented plasminogen activator inhibitor 1 (PAI-1) with PG/VG + nicotine exposure in mouse lungs. Lung inflammation is signified by acute lung injury biomarkers such as surfactant proteins, SP-A, SP-D, SP-B, and SP-C. These surfactant proteins lower the surface tension, preventing the alveolar from collapsing and play a critical role in the innate immune response. Thus, we determined the potential correlations of mechanisms of inflammatory and injurious responses by acute menthol and tobacco flavor exposure. Acute lung injury markers, NOD-, LRR-, and pyrin domain-containing protein 3 (NLRP3) inflammasome, surfactant protein D (SP-D), and plasminogen activator inhibitor 1 (PAI-1) were determined in mouse lungs post-exposure to e-cigs (Koivisto *et al.*, 2022; Moilanen *et al.*, 2012). As metabolic homeostasis has been shown to play a role in the incidence of asthma, we integrated innate and adaptive immune responses with cellular metabolism to understand the metabolic reprogramming of immune cells, which is essential for both inflammatory and antiinflammatory responses(Brumpton *et al.*, 2013; O'Neill, 2017; O'Neill *et al.*, 2016; Palsson-McDermott and O'Neill, 2020).

In this study, we hypothesized that both C57BL/6J and BALB/cJ mouse strains would elicit Th1 and Th2 inflammatory responses upon e-cigarette aerosol exposures, respectively. We also hypothesized that PG/VG, menthol, and tobacco flavors would cause differential proinflammatory and correlated acute phase responses regardless of brand differences, and that nicotine would exacerbate the inflammatory response.

Methods

Scientific rigor and reproducibility

We applied a robust, unbiased experimental design, and data analysis approach throughout the study. We validated the methods and ensured reproducibility with repeated experiments. All methods are presented in detail with transparency. Results were reported and interpreted without bias. For all assays, laboratory-grade biological and chemical resources were purchased from commercial sources. Our methodologies, data, and results adhered to strict NIH reproducibility standards and scientific rigor. Exposures had male and female mice of the same age, $N = 8$–10 per strain. For e-liquid exposures, instead of generalizing the effects with just one brand, we included two brands. All analytes were assayed with $N = 2$–3 technical replicates per group. Assays were performed with unique IDs and self-blinded to avoid bias.

Ethics statement: institutional biosafety and animal protocol approval

Experiments in this study were performed according to the standards and guidelines approved by The University of Rochester Institutional Biosafety Committee (study approval number: Rahman/102054/09-167/07-186; identification code: 07-186; date of approval: 5 January 2019 and 3 February 2020).

All mouse housing, handling, exposure, and procedure protocols used in this study were approved by the University Committee on Animal Research (UCAR) Committee of the University of Rochester, Rochester, NY (UCAR protocol 102204/UCAR-2007-070E, date of approval: January 5, 2019, and February 3, 2020).

Animals

For *in vivo* exposures, 8- to 10-week-old male and female C57BL/6J and BALB/cJ mice (body weight ~25 g) from Jackson labs were purchased and housed at the University of Rochester vivarium under normal light and dark cycles and *ad libitum* feeding according to UCAR guidelines.

Procurement of ENDS e-liquids

Two nationwide commercially available e-liquid brands were de-identified as A and B for propylene glycol (PG), vegetable glycerin (VG), menthol 0 mg nicotine, menthol with 6 mg nicotine, tobacco flavor 0 mg nicotine, and tobacco flavor with 6 mg nicotine procured from local vendors. E-liquids were stored in a dark room in a cooler until use. PG/VG (1:1) was prepared fresh before each exposure by mixing overnight on a rocker. Hence, the products were obtained from different vendors with matching humectants, nicotine, and flavors.

Characterization of liquid and vapor phase constituents

E-liquids (menthol and tobacco) were chemically characterized by gas chromatography and mass spectrometry (GC-MS). Aerosols from menthol and tobacco flavors were sampled in 1-l vacuum bottles, and each cartridge was sampled for 10 min with 10 puffs each. These samples were sent to ALS Environmental, CA, for analysis of constituents remaining in the vapor phase after storage and shipping were analyzed by EPA method TO-15,

which focuses on a standard suite of terpenes and volatile organic compounds (VOCs). In addition, a mass spectral library search was used for tentatively identified compounds.

Whole-body ENDS aerosol exposure

The whole-body mouse exposure was performed using the InExpose vaping system attached to a Joytech (eVIC VTCmini) (SCIREQ). The 3rd generation e-cig device was automatically triggered and controlled by the SCIREQ Flexiware software (Version 8.0). The e-cig exposure regimen was based on Behar topography, simulating realistic exposure of 2 puffs/min (70 ml puff volume, 2 s puff duration, 30 s inter-puff interval, bias flow of 2 l/min) for a total of 2 h exposure time for three consecutive days. The e-liquid heating temperate was set to 220°C (80 W and 11–15 mA) with a 0.15-ohm coil. Mice were placed inside the exposure chamber, and real-time humidity, oxygen, carbon dioxide, and ambient temperature (∼20°C) were automatically recorded and monitored (Table 1). Using qTRAK (TSI) real-time probes for carbon monoxide (CO) and VOCs were recorded (Table 1). Mouse numbers were designated into air (control), PG/VG (1:1), menthol 0 mg nicotine, menthol 6 mg nicotine, tobacco 0 mg nicotine, and tobacco 6 mg nicotine. Exposure to e-cig aerosols was conducted for three consecutive days, 2 h/day. Air (control) group mice went through the same procedure as other mice with clean tubing with bias air flow without any aerosol exposures, and they were housed in a clean-air room post-sham exposure. Each mouse group exposed to respective flavored aerosols had separate designated tubing and pump heads to avoid residual contamination from other flavors, and the mice were housed in a clean-air room postexposure. Two hours after the third day of exposure to aerosols, blood was collected by submandibular method for serum cotinine analysis. After the last day, approximately 24 h later, the mice were sacrificed and blood (by vena cava collection method), bronchoalveolar lavage fluid (BALF), and lung tissues were collected. Cotinine levels in serum were estimated by ELISA (CalBiotech, Cat No. CO096D) to ensure the absence or presence of nicotine exposure in menthol and tobacco flavors.

Bronchoalveolar lavage collection

Upon anesthesia, 0.6 ml of 0.9% NaCl saline solution was instilled 3 times (1.8 ml cumulative volume) into the trachea and the recovered BALF was centrifuged at 1000 rpm for 7 min. The acellular fraction of the BALF was stored at −80°C for cytokine analysis by Luminex assay. The pelleted cells were then used for flow cytometry analysis to obtain differential cell counts.

Immunoblot analyses

Approximately 30 mg of lungs were homogenized in RIPA lysis buffer using a magnetic bullet blender. Protein in lung homogenate samples was determined by BCA assay (Thermo Scientific, Cat No. 23227), and approximately 20 μg of total protein per well was loaded onto 8%–15% SDS polyacrylamide gels for protein separation by electrophoresis (SDS-PAGE). Separated proteins were electroblotted onto nitrocellulose transfer membranes (Bio-Rad, 1620112). Membranes were blocked with 5% nonfat dry milk (1 h ambient temp) and probed with 1:1000 TRPA1 (Invitrogen, PA588615), 1:1000 SP-D (Abcam, ab220422), 1:1000 PAI-1 (Abcam, ab182973), and NLRP3 (Abcam, ab210491) primary antibodies overnight at 4°C. Goat Anti-Rabbit IgG (H + L) secondary antibody was used at a dilution of 1:10 000. 1:5000 GAPDH (Abcam, ab9482) and 1:5000 β-actin (Abcam, ab20272) were used as loading controls for the normalization of target proteins during densitometry analysis.

Inflammatory mediators by Luminex assay

Fifty microliters of BALF or homogenized lung tissue were used with BioRad 23-plex-Group I kit to quantify secreted inflammatory mediators (BioRad Catalog No. M60009RDPD) according to the manufacturer's instructions. Briefly, capture antibody-coupled magnetic beads were added to the plate, followed by the addition of samples and the standards. After incubating, the detection antibody and streptavidin-PE were added. The appropriate number of washing steps and incubation steps were followed as instructed. After resuspending the sample in 125 μl of assay buffer, the plate was read on a FLEXMAP 3D system (Luminex, Austin, Texas). The concentrations of each analyte were compared to the unexposed air group and the analytes that showed significant differences were reported.

Genotoxicity assessment

To assess genotoxicity caused by ENDS exposures, frozen lung tissues were homogenized in RIPA buffer and the protein levels were determined by Pierce BCA assay (Thermofisher, 23227). Subsequently, ATR, Chk1, Chk2, H2A.X, MDM2, p21, and P53 protein levels were measured by the magnetic bead panel (Cell Signaling Multiplex Assay, 48-621MAG, EMD Millipore) on FLEXMAP 3D. The data were normalized by protein levels for each analyte and reported as net median florescence intensity.

Flow cytometry analysis

Collected cells from the BALF recovery were counted by acridine orange/propidium iodide (AO/PI) assay to obtain total cell counts. The cells were then blocked with anti-CD16/32 (Fc block) for 10 min. Followed by a PBS wash step, cells were stained with CD45, F4/80, Ly6B.2, CD4, and CD8 cell surface markers in the staining buffer to identify approximate counts of cell populations. After 30 min of incubation in the dark at 4°C, the cells were washed twice in PBS and resuspended in 100 μl buffer. Appropriate FMO controls and compensation beads were used for compensation. Sample acquisition was performed using a Guava easyCyte 8 flow cytometer (Luminex). Data analysis was performed using GuavaSoft 3.3.

Gene expression profiling by NanoString sprint profiler

RNA samples isolated using Direct-zol Zymo kit according to manufacturer's protocol from mouse lung lobes were quantified through NanoDrop spectrophotometer (ND-1000, NanoDrop

Table 1. Mouse exposure chamber conditions during aerosol exposures

	Temperature	RH%	CO (ppm)	CO$_2$	VOC (ppm)
PG/VG	21.38 ± 0.31	67.13 ± 19.47	33.00 ± 6.99	145.75 ± 159.22	13.33 ± 1.89
Menthol	21.85 ± 0.34	84.23 ± 8.56	2.99 ± 6.44	342.45 ± 327.98	46.55 ± 23.84
Menthol + Nic	21.74 ± 0.18	87.24 ± 21.57	0.52 ± 1.79	334.67 ± 310.92	29.67 ± 10.58
Tobacco	21.03 ± 0.43	74.55 ± 4.79	14.86 ± 15.14	14.92 ± 33.31	11.00 ± 8.50
Tobacco + Nic	21.78 ± 0.47	57.76 ± 7.07	21.86 ± 26.90	30.00 ± 38.92	15.46 ± 6.07
Overall	21.56 ± 0.35	74.18 ± 12.16	14.65 ± 13.46	173.56 ± 158.93	23.20 ± 14.94

Technologies), and 30 ng RNA samples were prepared for NanoString analysis. Premade NanoString codesets for metabolic and inflammation genes were purchased and hybridized with the samples according to the manufacturer's guidelines. Gene expressions were assessed after quality check and normalization using nSolver 4.0 software. Significantly upregulated genes ($p < .05$) curated and Venn diagram was prepared using https://bioinformatics.psb.ugent.be/webtools/Venn/

Proteomics analysis

Approximately 20 mg of snap-frozen mouse lungs were tested for suitability (no blood contamination) by hemoglobin SDS-PAGE and the provided Max Quant Log_2 fold change values were provided by the University of Rochester proteomics core facility.

In brief, protein extraction, protein concentration estimation, sample trypsinization, and S-Trap centrifugation were performed to collect the digested peptides. Subsequently, data collection performed for peptides from each fraction were injected onto a home-made 30 cm C18 column with 1.8 um beads (Sepax), with an Easy nLC-1200 HPLC (Thermo Fisher), connected to a Fusion Lumos Tribrid mass spectrometer (Thermo Fisher). Solvent A was 0.1% formic acid in water, while solvent B was 0.1% formic acid in 80% acetonitrile. Ions were introduced to the mass spectrometer using a Nanospray Flex source operating at 2 kV. The gradient began at 3% B and held for 2 min, increased to 10% B over 7 min, increased to 38% B over 64 min, then ramped up to 90% B in 5 min and was held for 3 min, before returning to starting conditions in 2 min and re-equilibrating for 7 min, for a total run time of 90 min. Raw data were processed with DIA-NN version 1.8.1 (https://github.com/vdemichev/DIA-NN). For all experiments, data analysis was carried out using library-free analysis mode in DIA-NN. To annotate the library, the mouse UniProt "one protein sequence per gene" database (UP000000589, downloaded 4/7/2021) was used with "deep learning-based spectra and RT prediction" enabled. Protein quantification carried out using the MaxLFQ algorithm as implemented in the DIA-NN R package (https://github.com/vdemichev/diann-rpackage) and the number of peptides quantified in each protein group was counted as implemented in the DiannReportGenerator Package (https://github.com/kswovick/DIANN-Report-Generator).

Subsequently, data for each exposure group (air, PG/VG, menthol, menthol 6 mg nicotine, tobacco, tobacco 6 mg nicotine) were curated to identify ±1.5-fold change. Data presented in a Venn diagram using https://bioinformatics.psb.ugent.be/webtools/Venn/

Mitochondrial bioenergetics of MLE15 cells treated with extracellular vesicles isolated from tobacco flavor exposed mouse lung

Murine type II epithelial cells (MLE-15) were cultured in DMEM/F12K medium and L2: F12K medium supplemented with 10% FBS, 2 mM L-glutamine, 100 IU/ml penicillin, and 100 µg/ml streptomycin at 37°C in a humidified atmosphere containing 5% CO_2 until confluency. Cells were seeded at 20 000 seeding density on 6-well seahorse plates (Cat No. 103025-100). We isolated exosomes, by digesting ~40 mg of lung tissue from mice exposed to tobacco flavor and air (control) groups in 1x Liberase, and sequentially centrifuging at 300 × g, 2000 × g, 10 000 × g, and finally at 100 000 × g via ultracentrifugation method. MLE cells in seahorse plates were then treated with isolated exosomes at 5 µg/ml. Twenty-four hours posttreatment, MitoStress assay (Cat No. 13015-100, Agilent) was performed per manufacturer's instructions to measure the extracellular acidification rate (ECAR) and oxygen consumption rate (OCR) of MLE cells upon treatment. The data were normalized by live cell count in each well and plotted by Wave software.

Statistical analysis

The statistical differences between treatment groups were analyzed through t-tests, one-way ANOVA, and two-way ANOVA in GraphPad Prism software (version 9). Results were presented as the mean ± SEM. A p-value of <.05 was considered significant.

Results

Chemical composition of menthol and tobacco flavors based on two e-liquid brands A and B

Chemical characterization of liquid and vapor phases showed high levels of alcohol-ethanol, PG, propene, 1,3-butadiene, acetone, acetaldehyde, propene, acrolein, methacrolein, sulfur dioxide, n-propanal, maltol, ethyl ether, menthanone, levomenthol, isoprene, ethyl acetate, alpha pinene, and beta pinene. Menthol derivatives were found in both tobacco and menthol flavors (Tables 2 and 3). Tobacco and menthol flavors had 33 common chemical constituents in the liquid phase and 82 common VOCs in the aerosol phase (Figures 1A and 1B). Further, we detected less than 1 mg/ml of nicotine in menthol and tobacco bottles labeled as zero nicotine. Our data suggest that similar flavors from different brands/vendors have an inconsistent formulation of chemicals attributable to the differences in the toxicological assessment. We confirmed nicotine exposure by measuring serum cotinine levels 2 h postexposure. In menthol 6 mg nicotine-exposed mice, the serum cotinine level was approximately 113 ng/ml and in the tobacco 6 mg nicotine group, the cotinine level was approximately 29 ng/ml. In contrast, 24 h postexposure significantly reduced serum cotinine levels (Figure 1C).

Acute exposure to brand A, PG/VG, menthol, and tobacco with and without nicotine, induced immune cell infiltration in BALF, irrespective of the mouse strain

To assess the elicited inflammatory response by exposure to ENDS, total cell counts and differential cell count were determined in BALF. Exposure to PG/VG, menthol 0 mg nicotine, and menthol 6 mg nicotine, all of which are from brand A e-liquid, caused significant immune cell influx in the lung as the total cell number has increased in both C57BL/6J and BALB/cJ strains compared to the air group (Figure 2A). BALF cells were constituted mostly of alveolar macrophages and a slight reduction was seen in C57BL/6J mice exposed to tobacco with nicotine (Figures 2C and 2D). Greater differential influxes in neutrophils were observed in flavor-exposed groups, particularly in BALB/cJ mice. Both PG/VG and menthol 0 mg nicotine exposure caused a significant influx up to 2.9% (by 60% increase) in neutrophils compared to the air group, particularly in BALB/cJ mice (Figures 2E and 2F). Overall, CD4 lymphocyte percentages were decreased in PG/VG, tobacco ± nicotine exposed groups compared to the air group (by 88% significant decrease in C57BL/6J mice) (Figures 2G and 2H). In both C57BL/6J and BALB/cJ mice, PG/VG, menthol ± nicotine groups significantly reduced Tc cells to 0.4% (reduced by 74% compared to the air group; Figures 2I and 2J). Overall, menthol flavor induced inflammatory influx in BALB/cJ mice, while tobacco flavor exposure affected C57BL/6J mice more. These data suggest that acute exposure to brand A, PG/VG tobacco menthol flavors ± nicotine, elicited an inflammatory response.

Table 2. Tobacco and menthol E-liquid flavor chemical constituents

Tobacco Flavor		Menthol Flavor	
CAS	Chemical Name	CAS	Chemical Name
54-11-5	Pyridine, 3-(1-methyl-2-pyrrolidinyl)-, (S)-	54-11-5	Pyridine, 3-(1-methyl-2-pyrrolidinyl)-, (S)-
4940-11-08 00:00:00	Ethyl maltol	4940-11-08 00:00:00	Ethyl maltol
71-55-6	Ethane, 1,1,1-trichloro-	71-55-6	Ethane, 1,1,1-trichloro-
623-37-0	Hexan-3-ol	623-37-0	Hexan-3-ol
1000152-79-7	Cyclopentane, 1,2,3,4,5-pentamethyl-	1000152-79-7	Cyclopentane, 1,2,3,4,5-pentamethyl-
26456-76-8	2-Hexene, 3,5,5-trimethyl-	26456-76-8	2-Hexene, 3,5,5-trimethyl-
75-85-4	Amylene hydrate	75-85-4	Amylene hydrate
40467-04-7	2-Hexene, 2,5,5-trimethyl-	40467-04-7	2-Hexene, 2,5,5-trimethyl-
693-65-2	Amyl ether	693-65-2	Amyl ether
110-98-5	2-Propanol, 1,1′-oxybis-	110-98-5	2-Propanol, 1,1′-oxybis-
1678-82-6	Menthane <trans-para->	1678-82-6	Menthane <trans-para->
116-09-6	Hydroxyacetone	116-09-6	Hydroxyacetone
2568-25-4	1,3-Dioxolane, 4-methyl-2-phenyl-	2568-25-4	1,3-Dioxolane, 4-methyl-2-phenyl-
60-12-8	Phenylethyl alcohol	60-12-8	Phenylethyl alcohol
104-67-6	2(3H)-Furanone, 5-heptyldihydro-	104-67-6	2(3H)-Furanone, 5-heptyldihydro-
78-70-6	Linalool	78-70-6	Linalool
98-55-5	Terpineol <alpha->	98-55-5	Terpineol <alpha->
104-76-7	1-Hexanol, 2-ethyl-	104-76-7	1-Hexanol, 2-ethyl-
121-33-5	Vanillin	1490-04-6	Menthol
118-71-8	Maltol	121-32-4	Vanillal
106-62-7	1-Propanol, 2-(2-hydroxypropoxy)-	14371-10-9	Cinnamaldehyde <(E)->
56-81-5	Glycerin	2890-62-2	Ethanone, 1-(1-methylcyclohexyl)-
6214-01-03 00:00:00	1,2-Propanediol, 2-acetate	563-80-4	2-Butanone, 3-methyl-
68527-74-2	Vanillin propylene glycol acetal	53951-43-2	1,3-Dioxolane-2-methanol,2,4-dimethyl-
706-14-9	2(3H)-Furanone, 5-hexyldihydro-	107-87-9	Propyl methyl ketone
100-51-6	Benzyl alcohol	7149-26-0	Linalyl anthranilate
106-61-6	1,2,3-Propanetriol, 1-acetate	80-71-7	2-Cyclopenten-1-one,2-hydroxy-3-methyl-
627-69-0	1,2-Propanediol, 1-acetate	765-70-8	Cyclopentane-1,2-dione <3-methyl->
1000378-33-1	1-[(1-Propoxypropan-2-yl)oxy]propan-2-yl acetate	928-96-1	Hex-(3Z)-enol
1754-62-7	2-Propenoic acid, 3-phenyl-, methyl ester, (E)-	67634-12-2	Lyral
102-62-5	Glycerol 1,2-diacetate	119-61-9	Benzophenone
1120-36-1	Tetradec-1-ene	84-66-2	Diethyl phthalate
102-76-1	Triacetin	928-97-2	3-Hexen-1-ol, (E)-
77-93-0	Triethyl citrate	54120-69-3	1,4-Dioxane-2,6-dimethanol
23726-91-2	Damascone <(E)-beta->	1319-88-6	Benzaldehyde glyceryl acetal
621-59-0	Benzaldehyde, 3-hydroxy-4-methoxy-	105-68-0	Propanoate <isopentyl->
1490-04-6	Cyclohexanol, 5-methyl-2-(1-methylethyl)-	556-52-5	Glycidol
121-32-4	Ethyl vanillin	106-27-4	Butanoic acid, 3-methylbutyl ester
14371-10-9	Cinnamaldehyde <(E)->	3623-51-6	Neomenthol
2890-62-2	Ethanone, 1-(1-methylcyclohexyl)-	491-07-6	Isomenthone
563-80-4	2-Butanone, 3-methyl-	7786-67-6	Isopulegol
53951-43-2	1,3-Dioxolane-2-methanol, 2,4-dimethyl-	15932-80-6	Pulegone
107-87-9	Propyl methyl ketone	470-82-6	Eucalyptol
7149-26-0	Linalyl anthranilate	51174-12-0	2,4,4-Trimethyl-1-hexene
80-71-7	2-Cyclopenten-1-one, 2-hydroxy-3-methyl-	584-03-2	1,2-Butanediol
765-70-8	Cyclopentane-1,2-dione <3-methyl->	1455-20-5	Butylthiophene <2->
928-96-1	Hex-(3Z)-enol	99-49-0	Carvone
67634-12-2	Lyral	16409-45-3	Cyclohexanol, 5-methyl-2-(1-methylethyl)-, acetate
119-61-9	Benzophenone	29141-10-4	(1R,2R,5S)-5-Methyl-2-(prop-1-en-2-yl)cyclo-hexanol
84-66-2	Diethyl phthalate	75-07-0	Acetic aldehyde
928-97-2	3-Hexen-1-ol, (E)-	6485-40-1	(−)-Carvone
65-85-0	Benzoic acid	15356-70-4	D(+) Menthol
120-57-0	Piperonal	1197-07-5	Carveol <trans->
97-54-1	Isoeugenol	14073-97-3	l-Menthone
97-53-0	Eugenol	589-98-0	3-Octanol
2051-49-2	Hexanoic acid, anhydride	4819-67-4	Delphone
6290-17-1	Ethyl acetoacetate propylene glycol ketal	2216-51-5	Levomenthol
93-58-3	Benzoic acid, methyl ester	89-81-6	2-Cyclohexen-1-one,3-methyl-6-(1-methyl-ethyl)-
554-12-1	Methyl propionate	89-82-7	Pulegone
68527-76-4	Ethylvanillin propylene glycol acetal, cis-	20405-60-1	Dihydrocarvyl acetate
123-11-5	Benzaldehyde, 4-methoxy-	112-30-1	Decyl alcohol
554-14-3	Thiophene <alpha-methyl->	2230-87-7	Neomenthyl acetate
120-51-4	Benzyl benzoate	3391-87-5	(+)-Menthone
166273-38-7	Pentanoic acid, 5-hydroxy-, 2,4-di-t-butyl-phenyl esters	104-46-1	Anethole

Table 2. (continued)

Tobacco Flavor		Menthol Flavor	
CAS	Chemical Name	CAS	Chemical Name
104-61-0	2(3H)-Furanone, dihydro-5-pentyl-	122-00-9	Acetophenone <4′-methyl->
584-02-1	Pentanol <3->	103-54-8	Acetic acid, cinnamyl ester
61683-99-6	1,3-Benzodioxole, 5-(4-methyl-1,3-dioxolan-2-yl)-	21040-45-9	Cinnamyl acetate <(E)->
134-20-3	Methyl anthranilate	52154-82-2	Mentha-2,8-dien-1-ol <trans-, para->
74421-06-0	2-Heptene, 5-ethyl-2,4-dimethyl-	127-91-3	Pinene <beta->
111-27-3	1-Hexanol	13877-93-5	Caryophyllene <(E)->
104-50-7	Octalactone <gamma->	1000155-47-0	3-Cyclohexen-1-one, 2-isopropyl-5-methyl-
616-44-4	Thiophene, 3-methyl-	4180-23-8	Anethole <(E)->
77-83-8	Ethyl 3-methyl-3-phenylglycidate (Z)	7212-40-0	2-Cyclohexen-1-ol,1-methyl-4-(1-methylethenyl)-, trans-
104-21-2	Benzenemethanol, 4-methoxy-, acetate	57-71-6	2,3-Butanedione, monooxime
105-13-5	Benzenemethanol, 4-methoxy-	1000364-16-7	3-Methylbenzyl alcohol, TBDMS derivative
76-09-5	2,3-Butanediol, 2,3-dimethyl-	1671-77-8	1-Pentanone, 1-(4-methylphenyl)-
106-24-1	Geraniol	35852-46-1	Pentanoate <cis-3-hexenyl->
105-21-5	2(3H)-Furanone, dihydro-5-propyl-	40625-96-5	5-Methyl-2,4-diisopropylphenol
19464-92-7	Ethyl methylphenylglycidate	1000400-22-0	4H-thiopyran-4-one, 2,3-dihydro-2-phenyl-
1126-51-8	5-Oxotetrahydrofuran-2-carboxylic acid, ethyl ester	1139-30-6	Caryophyllene oxide
10482-56-1	L-.alpha.-Terpineol	619-01-2	Cyclohexanol,2-methyl-5-(1-methylethenyl)-
17003-99-5	2-Nonene, 3-methyl-, (E)-	80-56-8	Pinene <alpha->
532-12-7	Pyridine, 3-(3,4-dihydro-2H-pyrrol-5-yl)-	118-65-0	Isocaryophyllene
7145-23-5	3-Hexene, 2,3-dimethyl-	18172-67-3	Bicyclo[3.1.1]heptane,6,6-dimethyl-2-methylene-, (1S)-
10473-13-9	3-Buten-2-ol, 2,3-dimethyl-	42436-07-7	cis-3-Hexenyl phenyl acetate
118-93-4	Acetophenone <2′-hydroxy->	50639-00-4	2-Hexen-1-ol, 2-ethyl-
2785-89-9	Phenol, 4-ethyl-2-methoxy-	1000145-04-8	1-Methyl-4-isopropyl-cyclohexyl 2-hydroperfluorobutanoate
486-56-6	Cotinine	1000139-76-4	Pentanoic acid, 4-methyl-, 1-buten-1-yl ester
614-97-1	5-Methylbenzimidazole	13466-78-9	3-Carene
92-48-8	2H-1-Benzopyran-2-one, 6-methyl-	149-57-5	Hexanoic acid <2-ethyl->
108-87-2	Hexahydrotoluene	4403-13-8	Ethylene glycol, TMS derivative
864685-64-3	2,3,4,4-Tetramethyl-5-methylidenecyclopent-2-en-1-one		
1000307-63-7	p-Anisic acid, 4-cyanophenyl ester		
1000343-91-2	Isophthalic acid, ethyl tridec-2-ynyl ester		
65079-19-8	6-Quinolinamine, 2-methyl-		
13588-28-8	1-Propanol, 2-(2-methoxypropoxy)-		
54644-41-6	Propanoic acid, 2,2-dimethyl-, 2-(1,1-dimethylethyl)phenyl ester		
7150-55-2	1-Butanone, 4-chloro-1-(4-hydroxyphenyl)-		

Exposure to brand A, PG/VG, menthol, and menthol with nicotine caused immunosuppression

Exposure to brand A, PG/VG, menthol 0 mg nicotine, and menthol 6 mg nicotine, caused highly significant suppression of major inflammatory cytokines, KC (Figure 3A, b), MIP-1α (Figure 3A, c), IL-1α (Figure 3A, j), IFNγ (Figure 3A, i), IL-1β (Figure 3A, m), IL-2 (Figure 3A, j), IL-3 (Figure 3A, g), IL-4 (Figure 3A, u), IL-5 (Figure 3A, k), IL-6 (Figure 3A, e), IL-9 (Figure 3A, s), IL-10 (Figure 3A, d), IL12 (p40) (Figure 3A, p), IL-12 (p70) (Figure 3A, q), IL-13 (Figure 3A, v), IL-17A (Figure 3A, h), Eotaxin (Figure 3A, i), G-CSF(Figure 3A, o), GM-CSF (Figure 3A, t), TNFα (Figure 3A, r), MIP-1β (Figure 3A, n), and MCP-1 (Figure 3A, w), in both C57BL/6J and BALB/cJ mouse BALF. However, RANTES levels were increased by menthol 0 mg nicotine exposure in both mouse strains but significantly in BALB/cJ (Figure 3A, a). However, this increase was reversed in the presence of nicotine (Figure 3A, a). In the lung homogenate, IL2 (NS), IL4 ($p < .05$), and IL9 ($p = .08$) were increased in C57BL/6J mice by 64%, 81%, and 50% increases respectively by exposure to menthol 0 mg ENDS flavor compared to the air group (Figures 3B, a–c).

Exposure to brand A, PG/VG, tobacco, and tobacco with nicotine caused cytokine suppression

PG/VG caused a nearly significant increase in TNFα ($p = .05$) (Figure 4R) and incremental nonsignificant increases in IL-1α (Figure 4J), IL-1β (Figure 4M), MIP-1β (Figure 4N), IFNγ (Figure 4L), GM-CSF (Figure 4O), IL17A (Figure 4H), IL5 (Figure 4K), and IL4 (Figure 4U) in BALB/cJ mice compared to C57BL/6J mice. Exposure to tobacco 0 mg, in general, caused immunosuppression significantly in C57BL/6J mice, including IL-1α (Figure 4J), IFNγ (Figure 4L), IL-1β (Figure 4M), GM-CSF (Figure 4O), IL4 (Figure 4U), IL-2 (Figure 4F), IL-3 (Figure 4G), IL-13 (Figure 4V), IL10 (Figure 4D), IL12p70 (Figure 4Q), IL12p40 (Figure 4P), IL9 (Figure 4S), and IL5 (Figure 4K) compared to the air group. In contrast, compared to the air group, tobacco 6 mg nicotine exposure significantly elevated levels of MIP-1α (Figure 4C) in both strains. Significant increases in RANTES (Figure 4A), IL-6 (Figure 4E), eotaxin (Figure 4I), and G-CSF (Figure 4T) were observed in C57BL/6J mice. This significantly suppressed cytokine response with the presence of nicotine demarcates the augmented response by flavor, which may be due to interaction with nicotine of the flavor alone.

**Table 3.** VOCs in tobacco- and menthol-flavored e-cigarette aerosols

Tobacco Flavor			Menthol Flavor		
CAS	Component	Conc (µg/m³)	CAS	Component	Conc. (µg/m³)
64-17-5	Ethanol	590 000	64-17-5	Ethanol	2 200 000
14073-97-3	l-Menthone	4400	67-64-1	Acetone	330 000
107-02-8	Acrolein	3500	107-02-8	Acrolein	150 000
75-07-0	Acetaldehyde	3100	75-07-0	Acetaldehyde	150 000
67-64-1	Acetone	2600	123-38-6	n-Propanal	77 000
57-55-6	Propylene glycol	1800	115-07-1	Propene	24 000
108-05-4	Vinyl acetate	1500	80-56-8	alpha-Pinene	7800
123-38-6	n-Propanal	1300	78-79-5	Isoprene	7000
107-18-6	2-Propen-1-ol	710	107-18-6	2-Propen-1-ol	7000
2216-51-5	Levomenthol	620	57-55-6	Propylene glycol	5600
67-63-0	2-Propanol (isopropyl alcohol)	600	108-05-4	Vinyl acetate	5100
460-00-4	Bromofluorobenzene	514	74-99-7	Propyne	5000
2037-26-5	Toluene-d8	507	127-91-3	beta-Pinene	4200
17060-07-0	1,2-Dichloroethane-d4	469	141-78-6	Ethyl acetate	3900
80-56-8	alpha-Pinene	430	115-11-7	2-Methylpropene	3900
75-15-0	Carbon disulfide	310	7446-09-5	Sulfur dioxide	2700
78-93-3	2-Butanone (MEK)	310	78-93-3	2-Butanone (MEK)	2500
141-78-6	Ethyl acetate	310	106-99-0	1,3-Butadiene	2300
110-82-7	Cyclohexane	310	78-84-2	2-Methylpropanal	2200
80-62-6	Methyl methacrylate	310	67-63-0	2-Propanol (isopropyl alcohol)	2000
179601-23-1	m,p-Xylenes	310	60-29-7	Ethyl ether	1800
100-44-7	Benzyl chloride	310	75-15-0	Carbon disulfide	1000
75-34-3	1,1-Dichloroethane	160	110-82-7	Cyclohexane	1000
109-99-9	Tetrahydrofuran (THF)	160	80-62-6	Methyl methacrylate	1000
123-86-4	n-Butyl acetate	160	179601-23-1	m,p-Xylenes	1000
115-07-1	Propene	150	100-44-7	Benzyl chloride	1000
75-71-8	Dichlorodifluoromethane (CFC 12)	150	75-34-3	1,1-Dichloroethane	520
74-87-3	Chloromethane	150	109-99-9	Tetrahydrofuran (THF)	520
76-14-2	1,2-Dichloro-1,1,2,2-tetra-fluoroethane (CFC 114)	150	123-86-4	n-Butyl acetate	520
75-01-4	Vinyl chloride	150	460-00-4	Bromofluorobenzene	517
106-99-0	1,3-Butadiene	150	75-01-4	Vinyl chloride	510
74-83-9	Bromomethane	150	74-83-9	Bromomethane	510
75-00-3	Chloroethane	150	75-00-3	Chloroethane	510
75-05-8	Acetonitrile	150	75-35-4	1,1-Dichloroethene	510
75-69-4	Trichlorofluoromethane	150	107-05-1	3-Chloro-1-propene (Allyl Chloride)	510
107-13-1	Acrylonitrile	150	76-13-1	Trichlorotrifluoroethane	510
75-35-4	1,1-Dichloroethene	150	156-60-5	trans-1,2-Dichloroethene	510
75-09-2	Methylene chloride	150	1634-04-4	Methyl tert-Butyl Ether	510
107-05-1	3-Chloro-1-propene (allyl chloride)	150	110-54-3	n-Hexane	510
76-13-1	Trichlorotrifluoroethane	150	67-66-3	Chloroform	510
156-60-5	trans-1,2-Dichloroethene	150	107-06-2	1,2-Dichloroethane	510
1634-04-4	Methyl tert-butyl ether	150	71-55-6	1,1,1-Trichloroethane	510
156-59-2	cis-1,2-Dichloroethene	150	78-87-5	1,2-Dichloropropane	510
110-54-3	n-Hexane	150	75-27-4	Bromodichloromethane	510
67-66-3	Chloroform	150	79-01-6	Trichloroethene	510
107-06-2	1,2-Dichloroethane	150	123-91-1	1,4-Dioxane	510
71-55-6	1,1,1-Trichloroethane	150	142-82-5	n-Heptane	510
71-43-2	Benzene	150	79-00-5	1,1,2-Trichloroethane	510
56-23-5	Carbon tetrachloride	150	108-88-3	Toluene	510
78-87-5	1,2-Dichloropropane	150	591-78-6	2-Hexanone	510
75-27-4	Bromodichloromethane	150	124-48-1	Dibromochloromethane	510
79-01-6	Trichloroethene	150	106-93-4	1,2-Dibromoethane	510
123-91-1	1,4-Dioxane	150	111-65-9	n-Octane	510
142-82-5	n-Heptane	150	108-90-7	Chlorobenzene	510
10061-01-5	cis-1,3-Dichloropropene	150	100-41-4	Ethylbenzene	510
108-10-1	4-Methyl-2-pentanone	150	75-25-2	Bromoform	510
10061-02-6	trans-1,3-Dichloropropene	150	95-47-6	o-Xylene	510
79-00-5	1,1,2-Trichloroethane	150	111-84-2	n-Nonane	510
108-88-3	Toluene	150	79-34-5	1,1,2,2-Tetrachloroethane	510
591-78-6	2-Hexanone	150	98-82-8	Cumene	510
124-48-1	Dibromochloromethane	150	103-65-1	n-Propylbenzene	510
106-93-4	1,2-Dibromoethane	150	622-96-8	4-Ethyltoluene	510
111-65-9	n-Octane	150	95-63-6	1,2,4-Trimethylbenzene	510
127-18-4	Tetrachloroethene	150	541-73-1	1,3-Dichlorobenzene	510
108-90-7	Chlorobenzene	150	106-46-7	1,4-Dichlorobenzene	510

(continued)

Table 3. (continued)

Tobacco Flavor			Menthol Flavor		
CAS	Component	Conc (μg/m³)	CAS	Component	Conc. (μg/m³)
100-41-4	Ethylbenzene	150	95-50-1	1,2-Dichlorobenzene	510
75-25-2	Bromoform	150	5989-27-5	D-Limonene	510
100-42-5	Styrene	150	120-82-1	1,2,4-Trichlorobenzene	510
95-47-6	o-Xylene	150	75-71-8	Dichlorodifluoromethane (CFC 12)	500
111-84-2	n-Nonane	150	74-87-3	Chloromethane	500
79-34-5	1,1,2,2-Tetrachloroethane	150	76-14-2	1,2-Dichloro-1,1,2,2-tetra-fluoroethane (CFC 114)	500
98-82-8	Cumene	150	75-05-8	Acetonitrile	500
103-65-1	n-Propylbenzene	150	75-69-4	Trichlorofluoromethane	500
622-96-8	4-Ethyltoluene	150	107-13-1	Acrylonitrile	500
108-67-8	1,3,5-Trimethylbenzene	150	75-09-2	Methylene chloride	500
95-63-6	1,2,4-Trimethylbenzene	150	156-59-2	cis-1,2-Dichloroethene	500
541-73-1	1,3-Dichlorobenzene	150	71-43-2	Benzene	500
106-46-7	1,4-Dichlorobenzene	150	56-23-5	Carbon tetrachloride	500
95-50-1	1,2-Dichlorobenzene	150	108-10-1	4-Methyl-2-pentanone	500
5989-27-5	D-Limonene	150	10061-02-6	trans-1,3-Dichloropropene	500
96-12-8	1,2-Dibromo-3-chloropropane	150	100-42-5	Styrene	500
120-82-1	1,2,4-Trichlorobenzene	150	108-67-8	1,3,5-Trimethylbenzene	500
91-20-3	Naphthalene	150	96-12-8	1,2-Dibromo-3-chloropropane	500
87-68-3	Hexachlorobutadiene	150	87-68-3	Hexachlorobutadiene	500
			2037-26-5	Toluene-d8	494
			10061-01-5	cis-1,3-Dichloropropene	490
			127-18-4	Tetrachloroethene	490
			91-20-3	Naphthalene	490
			17060-07-0	1,2-Dichloroethane-d4	475

A Liquid-phase chemical constituents

Tobacco / Menthol Venn diagram: 65, 33, 58
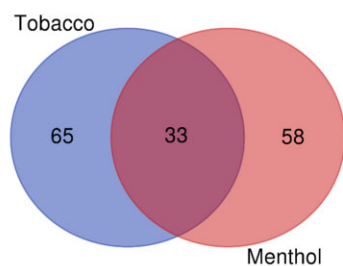
B Aerosol-phase Volatile Organic Compounds

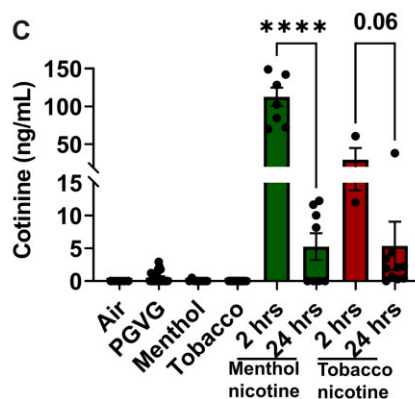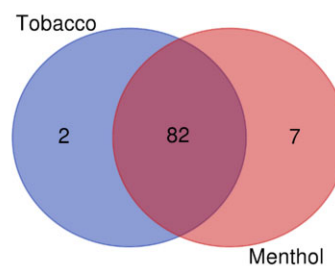Tobacco / Menthol Venn diagram: 2, 82, 7

C

Figure 1. A, Venn diagram depicting the number of detected chemicals tobacco and menthol flavors. E-liquids, tobacco and menthol, from two brands (A and B) were analyzed by GC-MS for their chemical composition. Tobacco and menthol flavors have distinctly 65 and 58 flavor constituents with 33 being common constituents. B, Venn diagram depicting the number of detected volatile organic compounds in tobacco and menthol flavored aerosols. Aerosols, tobacco and menthol, from two brands (A and B), were analyzed by GC-MS for their chemical composition. Tobacco and menthol flavors had two and seven constituents exclusively, with 82 being common overlapping constituents. C, Serum cotinine levels of mice exposed to menthol and tobacco aerosols with and without nicotine. Cotinine levels in serum quantified in C57BL/6J and BALB/cJ male and female mice exposed to air, PG/VG, menthol 0 and 6 mg nicotine, and tobacco 0 and 6 mg nicotine of brand A. Serum from menthol and tobacco groups with nicotine were collected at 2 and 24 h post 3-day exposure ($N = 3$–8 per group, ****$p < .0001$, t-test).
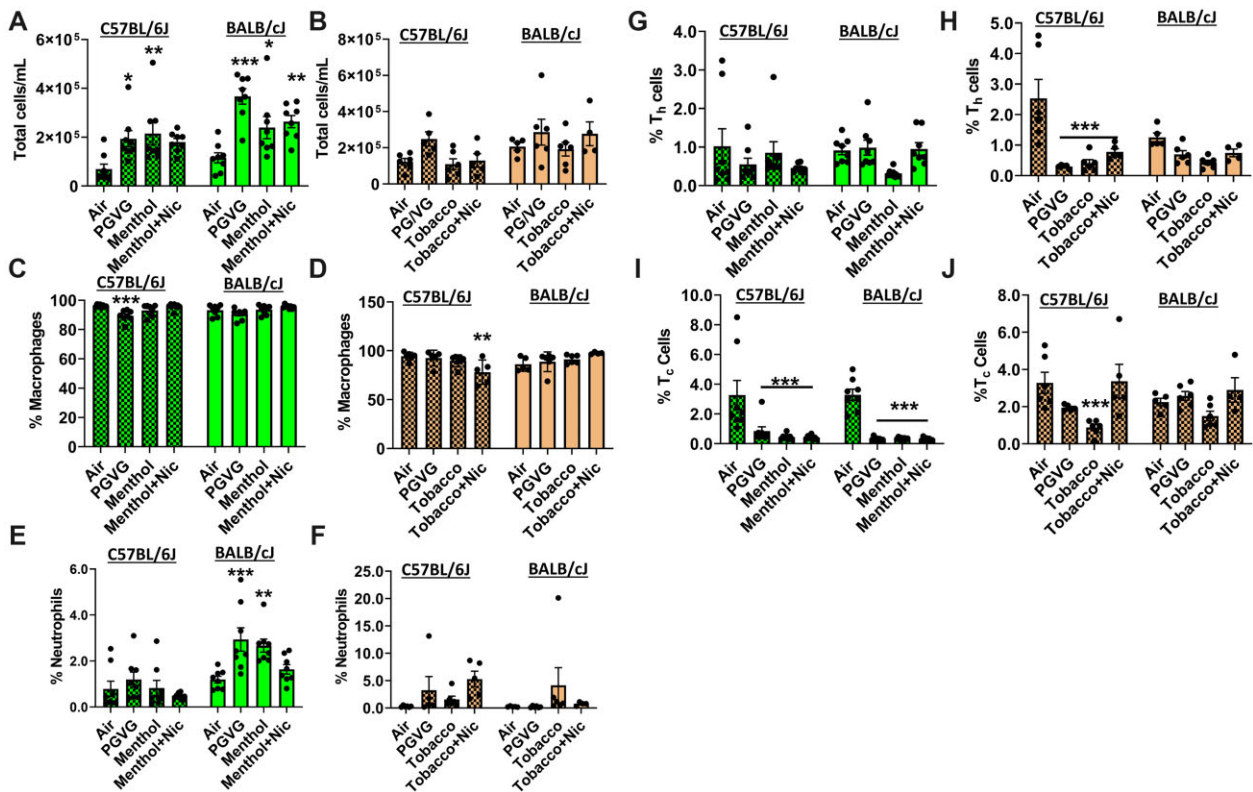
Figure 2. Differential cell counts in bronchoalveolar lavage fluid by exposure to brand A, PG/VG, menthol, and tobacco flavors with and without nicotine in C57BL/6J and BALB/cJ mice. C57BL/6J and BALB/cJ male and female mice were exposed to PG/VG, menthol, menthol 6 mg nicotine, tobacco, and tobacco 6 mg nicotine 2 h/day for three consecutive days in SCIREQ whole-body exposure chamber. Mice were euthanized ~24 h postexposure and the BALF was collected. A and B, Total cell counts were performed by staining with AO/PI dye. C and D, Macrophages (F4/80+), E and F, neutrophils (Ly6B.2), G and H, Th lymphocytes (CD4+), and I and J, Tc lymphocytes (CD8+) were assessed as percentages of CD45+ parent cell population by flow cytometry. Data are shown as mean ± SEM. *$p < .05$, **$p < .01$, and ***$p < .001$ versus respective air group per strain (2-way ANOVA) ($N = 4$–8 per group).

These data suggest that while there are some differences in the immune response between the strains, overall, a similar inflammatory response was elicited by brand A, PG/VG, tobacco, and tobacco with nicotine in both strains. The interaction of nicotine with tobacco demonstrated an altered response. These responses are driven toward allergic inflammation and acute lung injury in the presence of nicotine and tobacco flavor.

Acute exposure to brand B, PG/VG, menthol, and tobacco flavors induced immune cell infiltration in BALF

To elucidate the flavor-specific immune response, an identical 3-day exposure to PG/VG, menthol, and tobacco without any nicotine from brand B was performed on C57BL/6J mice and the BALF differential cell counts were performed. Compared to the unexposed counterparts, the PG/VG-exposed mice had increased neutrophils (Ly6.b+) ($p < .05$), CD4 T-cells (NS), and CD8-T-cells ($p < .001$) compared to the air group (Figures 5A, b–d). Menthol flavor exposed groups had significantly increased neutrophils and both CD4 and CD8 T-lymphocytes (Figures 5A, c and d). In contrast, tobacco flavor exposure did not cause any changes in macrophage, neutrophil, or T-lymphocyte counts in BALF compared to the air group (Figures 5A, a–e). These data demonstrate that PG/VG and menthol from brand B caused a greater immune cell influx and an immune response compared to the tobacco flavor and air groups.

Exposure to brand B nicotine-free menthol flavor induced immune suppression

To further recapitulate the menthol and tobacco flavor-specific immune response, BALF from C57BL/6J mice exposed to brand B aerosols of PG/VG, menthol, and tobacco, were evaluated for inflammatory mediators. While most cytokines were not changed (data not shown), menthol flavor caused significant attenuation of MIP-1β, IL-12p40, IL-12p70, and IL3 (Figures 5B, a–d). Albeit not significant, IFNγ ($p = .05$), IL4, IL10, and GM-CSF levels were attenuated by the menthol exposure compared to the air control group (Figures 5B, g–j). Similar to the response elicited by brand A, RANTES levels were significantly elevated ($p < .001$) by brand B menthol flavor-exposed mice (Figure 5B, a). Furthermore, IL-6 levels were significantly elevated ($p < .001$) by menthol exposure (Figure 5B, f). These increased IL-6 and RANTES levels, along with decreased proinflammatory cytokines, suggest the inflammatory response may be allergic and immunosuppressive.

Exposure to menthol flavor-induced chemosensory cation channel TRPA1 and nicotine-augmented biomarkers of acute lung injury

TRPA1 abundance was significantly increased by PG/VG and menthol compared to the air group. In contrast, menthol 6 mg nicotine group TRPA1 level was reduced/inhibited compared to the menthol group reversing its level similar to the air group (Figure 6A) with full blots (Supplementary Figure 1). NLRP3 inflammasome was altered by menthol exposure (Figure 6B) with
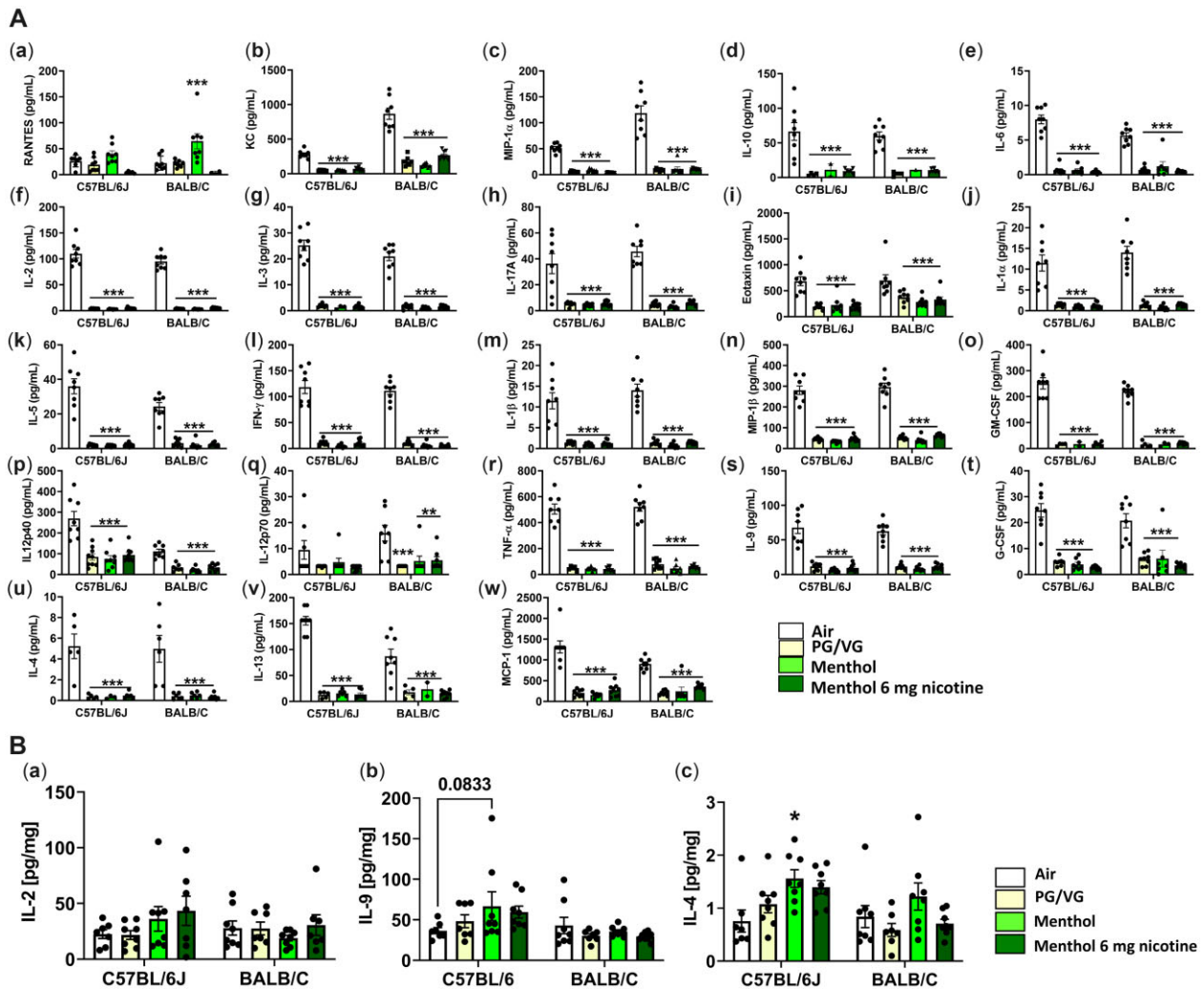
Figure 3. A, Exposure to brand A, PG/VG, menthol, and menthol with nicotine flavors in C57BL/6J and BALB/cJ mice elicited a regulatory inflammatory cytokine response in bronchoalveolar lavage. C57BL/6J and BALB/cJ, male and female, mice were exposed to PG/VG, menthol, and menthol 6 mg nicotine, 2 h/day for three consecutive days in SCIREQ whole-body exposure chamber. Mice were euthanized ~24 h postexposure and bronchoalveolar lavage was collected by instilling 0.6 ml 3× and pooled. Cytokine levels were measured by Luminex. a, RANTES; b, KC; c, MIP-1α; d, IL-10; i, IL-6; f, IL2; g, IL-3; h, IL-17A; i, Eotaxin; j, IL-1α; k, IL5; l, IFNγ; m, IL-1β; n, MIP-1β; o, GM-CSF; p, IL12p40; q, IL12p70; r, TNFα; s, IL9; t, G-CSF; u, IL-4; v, IL-13; w, MCP-1. Data are shown as mean ± SEM. *$p < .05$, **$p < .01$, ***$p < .001$ versus respective air group per strain (2-way ANOVA) ($N = 7$–8 per group). B, Exposure to brand A, PG/VG, menthol, and tobacco flavors with and without nicotine in C57BL/6J and BALB/cJ mice elicited a cytokine response in mouse lung homogenate. C57BL/6J and BALB/cJ, male and female, mice were exposed to PG/VG, menthol, menthol 6 mg nicotine, tobacco, and tobacco 6 mg nicotine 2 h/day for three consecutive days in SCIREQ whole-body exposure chamber. Mice were euthanized ~24 h postexposure and lung tissues were collected. Homogenized lungs in RIPA buffer were used to determine inflammatory mediators by Luminex and normalized by total protein (BCA assay). a, IL-2; b, IL-9; c, IL-4. Datat are shown as mean ± SEM. *$p < .05$ versus respective air group per strain (2-way ANOVA) ($N = 7$–8 per group).

full blot (Supplementary Figure 2). Surfactant protein SP-D was significantly reduced by menthol 6 mg nicotine exposure group (Figure 6C) with full blot (Supplementary Figure 2). While PAI-1 level was significantly reduced by tobacco 0 mg nicotine, this was reversed in the presence of nicotine, augmenting the PAI-1 protein abundance significantly (Figure 6D) with full blot (Supplementary Figure 1). Data suggest exposure to PG/VG and flavors with nicotine may cause acute lung injury (Figures 6B–D).

Exposure to PG/VG, menthol, and tobacco flavors caused genotoxicity

Genotoxicity markers by acute exposure to brand A aerosols (flavors sold as 0 and 6 mg nicotine) and brand B aerosols (flavors are nicotine-free) were determined in mouse lung tissue. Brand B PG/VG exposure caused a significant increase in p21 and ATR (Figures 7C and D). Mice exposed to menthol (0 mg nicotine)

increased H2A.X, MDM2, and p21 significantly (Figures 7A–C). Mice exposed to tobacco 0 mg nicotine caused a significant increase in p21 by brand B aerosol exposure (Figure 7C). Tobacco (0 mg nicotine brand B) increased p21 levels while brand A tobacco flavor with 6 mg nicotine increased H2A.X levels (Figures 7A and C). Overall, aerosols (PG/VG, menthol, tobacco with and without nicotine), demonstrated significantly altered genotoxic parameters while there were differences between brand, flavor, and the presence of nicotine (Figure 7). These data suggest that acute exposure to e-cig aerosols may cause genotoxicity.

Exposure to aerosols-induced intracellular p38-p70s6k kinase-associated signaling

To determine potential pathways of intracellular signaling upon exposure to nicotine-free brand B ENDS aerosols, prepared cell lysates were assessed for major signaling receptor tyrosine
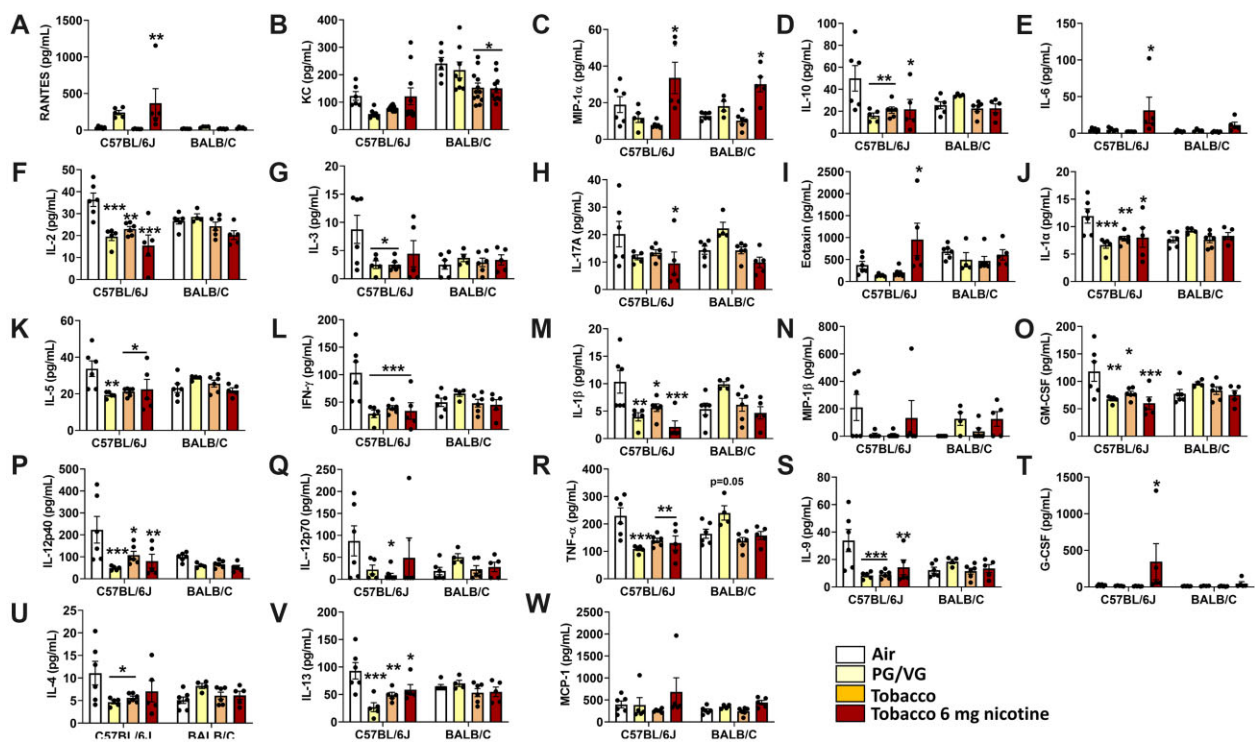
Figure 4. Exposure to brand A, PG/VG, tobacco, and tobacco with nicotine flavors in C57BL/6J and BALB/cJ mice elicited a regulatory inflammatory cytokine response in bronchoalveolar lavage. C57BL/6J and BALB/cJ, male and female mice, were exposed to PG/VG, tobacco, and tobacco 6 mg nicotine 2 h/day for three consecutive days in SCIREQ whole-body exposure chamber. Mice were euthanized ∼24 h postexposure and bronchoalveolar lavage was collected by instilling 0.6 ml 3× and pooled. Cytokine levels were measured by Luminex. A, RANTES; B, KC; C, MIP-1α; D, IL-10; E, IL-6; F, IL2; G, IL-3; H, IL-17A; I, Eotaxin; J, IL-1α; K, IL5; L, IFNγ; M, IL-1β; N, MIP-1β; O, GM-CSF; P, IL12p40; Q, IL12p70; R, TNFα; S, IL9; T, G-CSF; U, IL-4; V, IL-13; W, MCP-1. Data are presented as mean ± SEM. $^*p < .05$, $^{**}p < .01$, and $^{***}p < .001$ versus respective air group per strain (2-way ANOVA) (N = 7–8 per group).

kinases, which are key for cellular metabolism. PG/VG significantly elevated p70S6K, JNK, Akt, and p38 (Figures 8A–D). Menthol and tobacco flavors significantly increased P70S6K and p38 protein levels (Figures 8A and D). Overall, p70S6K and p38 were increased by all aerosols (Figures 8A and D).

Acute exposure to PG/VG, menthol, and tobacco caused gene alterations related to immunometabolism

Lung tissues of C57BL/6J from acute exposure to PG/VG, menthol, and tobacco flavors from both brands of e-liquids were assessed for gene expression changes related to inflammation and metabolism. After individually analyzing each flavor exposed group, 22 genes that changed significantly ($p < .05$) by acute exposure to ENDS aerosols compared to the air group were identified. These genes include Uck1, Mapt, Csf2, Ercc6, Abl1, Rps6kb1, Sod3, Kat6a, Atxn7, Ampd2, Pi3kr, Zfp869, Col6a3, Cfd, Pi3kcb, Hspa2, Acadl, Atf4, H2-T23, Ash1, Ldh3a, and Clock. Individually PG/VG, tobacco, tobacco + Nic, menthol, and menthol + Nic groups dysregulated 52,134, 2,14, and 42 genes, respectively, and altered 22 commonly overlapped genes by all exposures, as depicted in a Venn diagram (Figure 9A). These genes are involved in metabolism, DNA damage response, oxidative stress, and tumor suppression/cell division homeostasis.

Acute exposure to PG/VG, menthol, and tobacco altered key acute phase and metabolic proteins

Mouse lungs analyzed for protein alterations upon each exposure to PG/VG, menthol 0 mg nicotine, menthol 6 mg nicotine, tobacco 0 mg, and tobacco 6 mg were curated in a Venn diagram to identify commonly altered proteins at least 1.5-fold by exposure to all aerosols as well as individual flavor for brand A. Serpin3a, Myl1, and Hbb-b2 proteins were altered by flavors (Figure 9B).

Treatment of MLE cells from extracellular vesicles isolated from mice exposed to tobacco flavor caused alterations in mitochondrial bioenergetics

As the acute exposure to flavors caused significant alterations in genes related to cellular metabolism, mitochondrial respiration of MLE cells treated with exosomes isolated from air and tobacco groups was assessed. We assessed the size of isolated exosomes, which were about 100–125 nm. Twenty-four hours after exosome treatment, MLE cells treated with exosomes derived from tobacco flavor exposed mice (Figure 10B) showed significantly lower OCR and ECAR compared to exomes derived from the air/control mice (Figure 10A). These data suggest that exosome cargo from tobacco-exposed mice may contain metabolic abrogating miRNA or proteins.

Immunometabolism-associated signaling by ingenuity pathway analysis

Core analysis of proteomics data by ingenuity pathway analysis (IPA) trial version (Krämer *et al.*, 2014) from menthol 0 mg nicotine-exposed mice showed inhibition and deactivation pathways of proinflammatory transcription factors (NOS2, RAPTOR signaling) and increased negative regulators such as serpins (Figure 11).
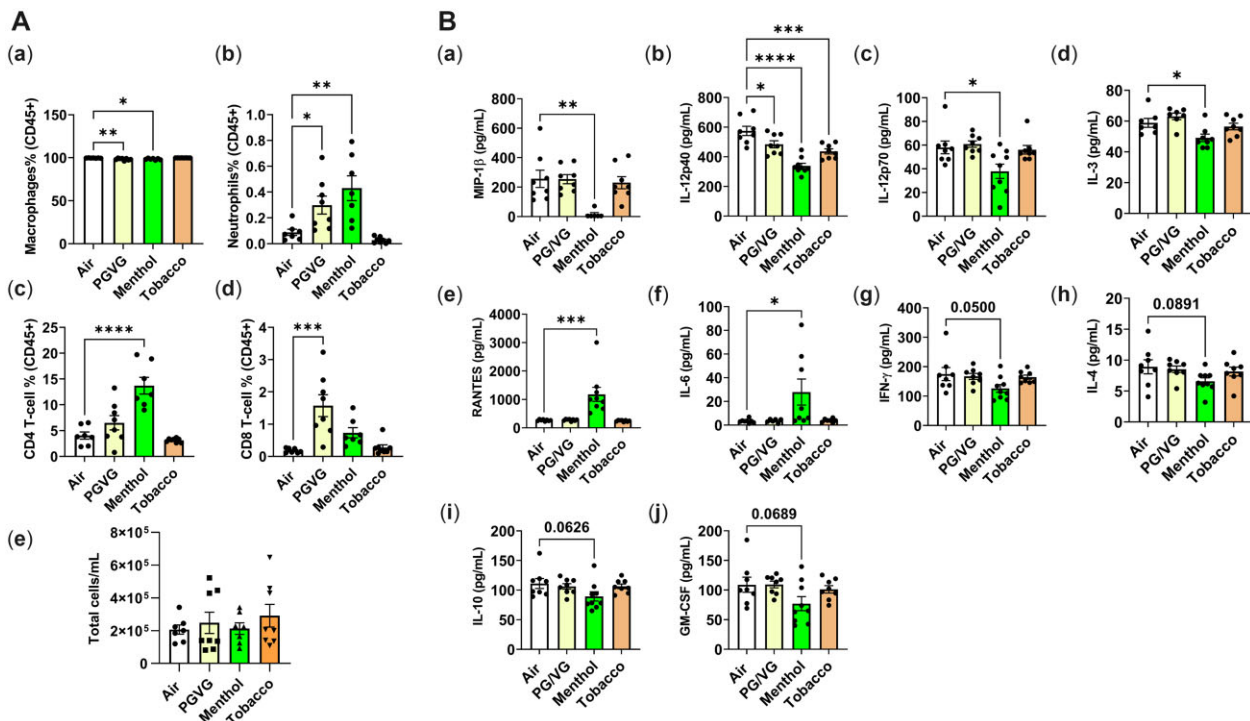
Figure 5. A, Differential cell counts in bronchoalveolar lavage by exposure to brand B, PG/VG, menthol, and tobacco flavors in C57BL/6J. C57BL/6J male and female mice were exposed to PG/VG, menthol, menthol 6 mg nicotine, tobacco, and tobacco 6 mg nicotine 2 h/day for three consecutive days in SCIREQ whole-body exposure chamber. Mice were euthanized ~24 h postexposure and the BALF was collected. a, Macrophages (F4/80+); b, neutrophils (Ly6B.2); c, Th lymphocytes (CD4+); d, Tc lymphocytes (CD8+), were assessed as percentages of CD45+ parent cell population by flow cytometry based on the (e) total cell counts determined by staining with AO/PI dye. Data are shown as mean ± SEM. $^*p < .05$, $^{**}p < .01$, $^{***}p < .001$ versus respective air group per strain (2-way ANOVA) (N = 8 per group). B, Exposure to brand B, PG/VG, menthol, and tobacco flavors in C57BL/6J mice elicited a differential inflammatory cytokine response in bronchoalveolar lavage. C57BL/6J male and female mice were exposed to PG/VG, menthol, menthol 6 mg nicotine, tobacco, and tobacco 6 mg nicotine 2 h/day for three consecutive days in SCIREQ whole-body exposure chamber. Mice were euthanized ~24 h postexposure and bronchoalveolar lavage was collected by instilling 0.6 ml 3× and pooled. Cytokine levels were measured by Luminex. a, MIP-1β; b, IL-12p40; c, IL-12p70; d, IL-3; e, RANTES; f, IL-6; g, IFNγ; h, IL-4; i, IL-10; j, GM-CSF. Data are shown as mean ± SEM. $^*p < .05$, $^{**}p < .01$, $^{***}p < .001$, and $^{****}p < .0001$ versus respective air group per strain (2-way ANOVA) (N = 8 per group).

Discussion

According to a 2018–2019 tobacco user survey, over 23.1% of e-cigarette users were never smokers (Mayer *et al.*, 2020). In this study, using an *in vivo* mouse exposure model, we conducted an acute exposure to ENDS aerosols to determine the inflammatory response, genotoxicity, and metabolic changes in the lung, simulating the inhalation toxicological effects of a nonsmoker response to first-time acute e-cig exposure (naïve exposure). The acute phase immune response and its resolution upon exposure to carrier fluid/humectant (PG/VG), menthol, and tobacco flavors with and without nicotine from different brands has been demonstrated in this study. We hypothesized that a proinflammatory response would be elicited upon exposure to aerosols, and the two brands would be consistent or differential in their responses to PG/VG, menthol, and tobacco with and without nicotine flavors aerosol exposures.

In our tested tobacco and menthol flavored product chemical analysis, we determined that flavored e-liquids contain a mixture of chemicals, including significant overlap in liquid and aerosol phase constituents. Therefore, it must be noted that the toxicity and biological responses result from these chemical constituents and is not attributable to a certain flavor *per se*. The additive or synergistic toxicity and effects of these chemicals in the flavors are important to be determined.

We observed cell infiltration in BALF by all flavors of both brands A and B. Among the BALF leukocytes, an increase in

neutrophils (significantly with menthol) and differential CD4 and CD8 counts were seen by brand A and B flavors. Small changes in neutrophilic cellular patterns may still mean great biological significance as greater than 3% can suggest collagen vascular diseases, IPF, aspiration pneumonia, infections, bronchitis, acute respiratory disease syndrome, and diffused-alveolar damage (Meyer *et al.*, 2012). There was a decrease in T lymphocytes with the exposure to brand A and an increase in CD4-T cell counts by brand B. Interestingly, all inflammatory mediators were suppressed by brand A PG/VG, menthol, and menthol 6 mg nicotine, except RANTES. While the same brand tobacco flavor exposure resulted in similar immunosuppression, tobacco with nicotine elevated G-CSF, RANTES, IL-6, MIP1α, and eotaxin levels. This suggests that though most inflammatory mediators were suppressed, there was an inflammatory response and the potential of nicotine interaction with flavors to augment the immune response. According to Alam *et al.*, asthmatic patients are often seen with increased MCP-1, RANTES, and MIP-1α levels in BALF (Alam *et al.*, 1996). Upregulation of RANTES mRNA and an increase in RANTES protein levels in asthmatics has been demonstrated, suggesting an association between RANTES expression and eosinophilia in asthma and allergic disease (Koya *et al.*, 2006). The response we observed with increased RANTES and intricacies of other inflammatory mediators associated with flavored aerosols-induced dampened proinflammation is consistent with recent studies that have demonstrated the T-lymphocytic correlation in the resolution of allergic asthma in mice exposed to
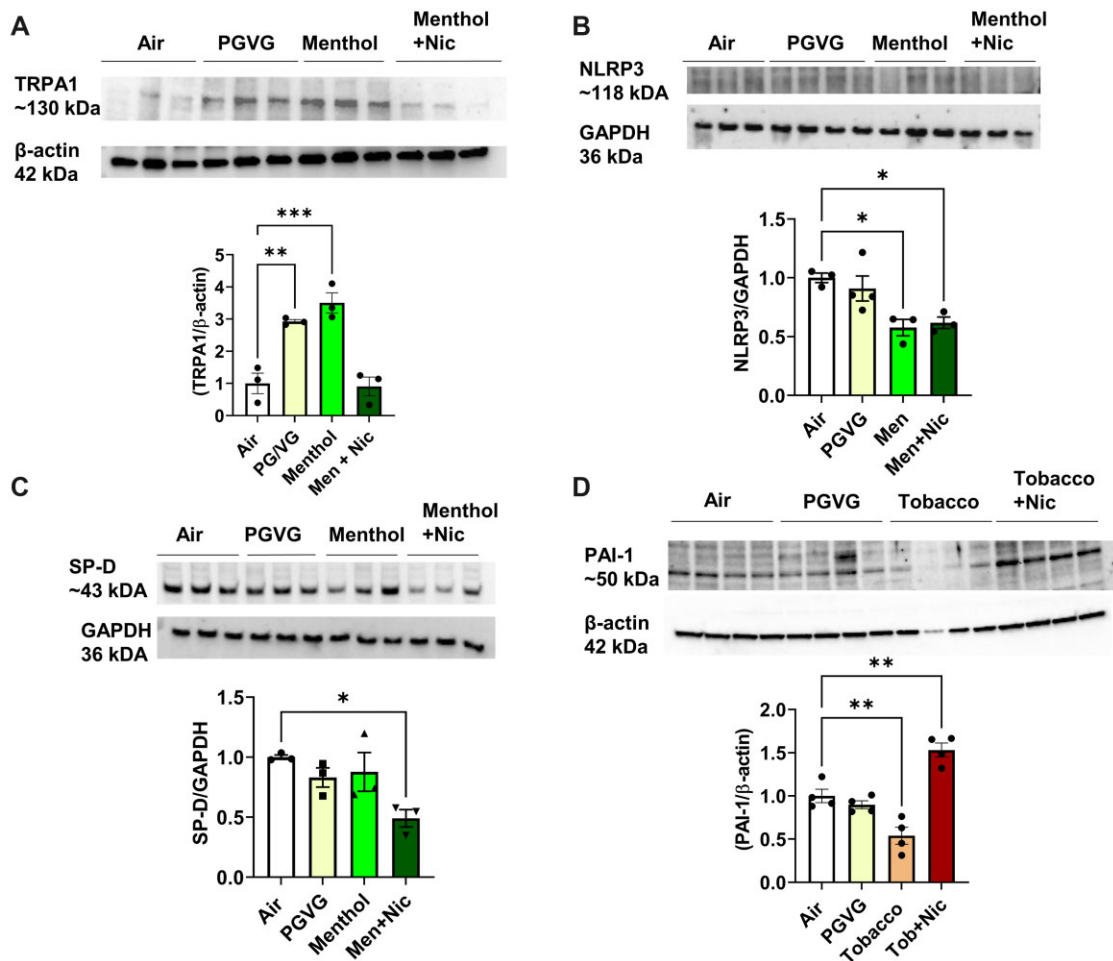
Figure 6. ENDS flavors induced acute lung injury-associated biomarkers. C57BL/6J male and female mice were exposed to PG/VG, menthol, menthol 6 mg nicotine, tobacco, and tobacco 6 mg nicotine 2 h/day for three consecutive days in SCIREQ whole-body exposure chamber. Mice were euthanized ~24 h postexposure, and lung tissues were homogenized for immunoblotting by SDS-PAGE. A, TRPA-1; B, NLRP3; C, SP-D; D, PAI-1 protein abundance were measured and normalized to GAPDH and β-actin loading controls. Data shown for respective bands and the densitometry values were plotted as mean ± SEM. $^*p < .05$, $^{**}p < .01$, and $^{***}p < .001$ versus respective air group per strain (2-way ANOVA) ($N = 3$–4 per group).

house dust mites (Li *et al.*, 2021a). Consistent with the inflammatory response, proteomics analysis showed a 3.2-fold increase of Muc5b levels in menthol flavor-exposed mice, indicating potential mucociliary dysfunction (Hancock *et al.*, 2018).

With brand A, PG/VG showed some elevated proinflammatory cytokines, such as increased TNFα in BALB/cJ group, though the increases were not significant in other mediators. This augmented response was unique to BALB/cJ mice. These small but differential changes in the PG/VG exposure may be attributed to PG/VG batch differences and chamber/coil heating conditions. Overall, exposure to brand A, PG/VG, menthol, and tobacco, demonstrated a controlled inflammatory response leaning toward immunosuppression or immune tolerance. Consistent with the results and the inflammatory changes observed in this study, regulatory processes, such as immunometabolism are critical to maintaining the homeostasis of an immune response (Chou *et al.*, 2022; Gotts *et al.*, 2019; Lloyd and Murdoch, 2010; Martin *et al.*, 2016). For the comparative analysis of the same flavor manufactured by 2 different brands, brand B flavor exposures were conducted. In PG/VG, menthol, and tobacco-exposed mice, there was a significantly increased neutrophil and CD4-T cell count compared to the air group. While PG/VG and tobacco exposures did not elicit any significant inflammatory cytokine response,

menthol exposure caused a significant attenuation in MIP-1β, IL-12p40, and IL12-p70, and a highly significant increase in IL-6 and RANTES levels. These changes once again suggest that there may be an allergic inflammatory response upon exposure to brand B, PG/VG, and menthol flavors, as these immune phenomena have been exemplified by IL-6 mediated asthma/allergic diseases (Neveu *et al.*, 2010; Rincon and Irvin, 2012). Overall, acute e-cig aerosol exposure elicited an immune response demonstrating a tolerogenic response with significant immune dampening.

Exposure to menthol flavor significantly increased TRPA1, which has been shown to play a role in response to exogenous irritants such as acrolein, cinnamaldehyde, and capsaicin. Consistent with our study, TRPA1 has been shown to play a complex role in basal airway function regulation, inflammatory mechanisms, and acute lung injury (Birrell *et al.*, 2009; Caceres *et al.*, 2009; Hajna *et al.*, 2020; Koivisto *et al.*, 2022; Moilanen *et al.*, 2012). With aerosol exposures, a reduction of surfactant protein D (SP-D) was seen, and SP-D has been shown to directly modulate innate immune cell function, pulmonary inflammation, and migration of peripheral monocyte/macrophages into the lung through GM-CSF–dependent pathways during indirect lung injury (King and Kingma, 2011). Further, this may explain slight but
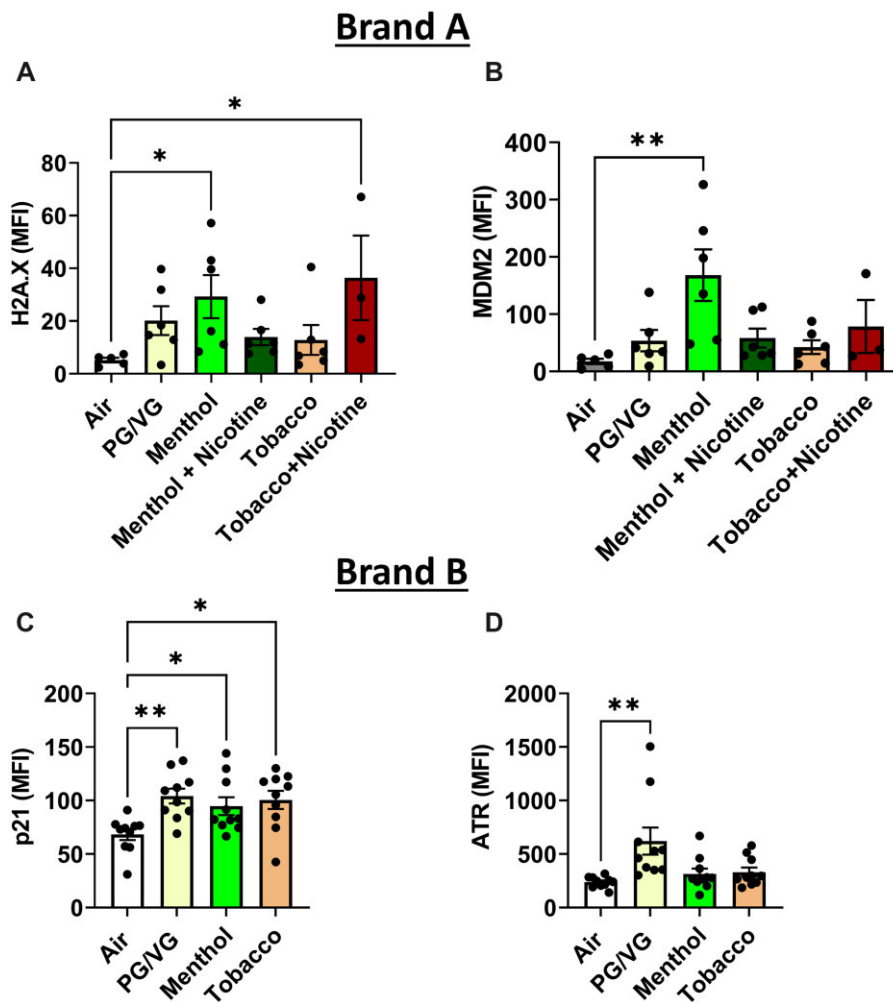
Brand A

Brand B

Figure 7. Genotoxicity by exposure to PG/VG, menthol, and tobacco flavors in C57BL/6J mouse lung tissue. C57BL/6J male and female mice were exposed to PG/VG, menthol, menthol 6 mg nicotine, tobacco, and tobacco 6 mg nicotine 2 h/day for three consecutive days in SCIREQ whole-body exposure chamber. Mice were euthanized ~24 h postexposure and mouse lung tissues were homogenized and measured genotoxicity markers, A, H2AX; B, MDM2; C, p21; and D, ATR by measuring net median florescence intensity (MFI) normalized to total protein. Data are shown as mean ± SEM. $^*p < .05$, $^{**}p < .01$, and $^{***}p < .001$ versus respective air group per strain (1-way ANOVA) ($N = 3$–10 per group).

significant changes in BALF macrophages in flavor aerosol-exposed mice. Further, tobacco-flavored nicotine-containing aerosol exposure caused a PAI-1 abundance increase in the lung tissues. Nicotine has been shown to increase PAI-1 and to have a direct causal effect in acute lung injury edema fluid-associated mortality (Prabhakaran et al., 2003; Zidovetzki et al., 1999).

Menthol and menthol with nicotine altered NLRP3 inflammasome protein abundance in mice. This is consistent with the immunosuppressive effects and immunomodulatory pathways we identified. NLRP3 inflammasome is the most prominent inflammasome promoting innate and adaptive immune responses and has been seen to destabilize by ubiquitination with cigarette smoke (Han et al., 2017). Growing evidence indicates that NLRP3 may create a metabolic loop in which glycolysis is induced upstream and downstream of NLRP3 inflammasome activation, corroborating the immunometabolic response upon exposure to aerosols in this study (Chou et al., 2022; Finucane et al., 2019).

Further, in the assessment of genotoxicity by brand A menthol and tobacco with nicotine exposures, DNA damage marker H2A.X protein levels were significantly increased. As H2AX

formation is intertwined with kinases such as ATM and ATR, it is plausible for the response to be PI3K mediated (Kuo and Yang, 2008; Marechal and Zou, 2013; Ward and Chen, 2001). MDM2, the primary negative regulator of p53, was significantly elevated by all aerosols, PG/VG, menthol and tobacco. This suggests MDM2-p53 may play a critical role in long-term exposure to these flavored ENDS in tumorigenesis, as p53 suppression has been associated with non-small-cell lung cancer (Deben et al., 2016, 2015). We observed significantly elevated levels of p70s6k, a serine/threonine kinase downstream target of mTOR. The mammalian target of rapamycin (mTOR) is pivotal for cellular nutrient processing, anabolic and catabolic homeostasis, and autophagy (Sabatini, 2017). Thus, the increase in p70s6k suggests mTOR involvement in the immunometabolic response we observed. Sinclair et al. demonstrated the function of mTOR in allergic inflammation by mediating the metabolic adaptation of such tissue-resident antigen-presenting cells and the immunological function of allergic inflammation (Sinclair et al., 2017; Wang and Wu, 2018). Our data suggest that aerosol exposure has resulted in an immunological defense and dormancy state due to mTORs mediated immunometabolic processes is consistent with existing
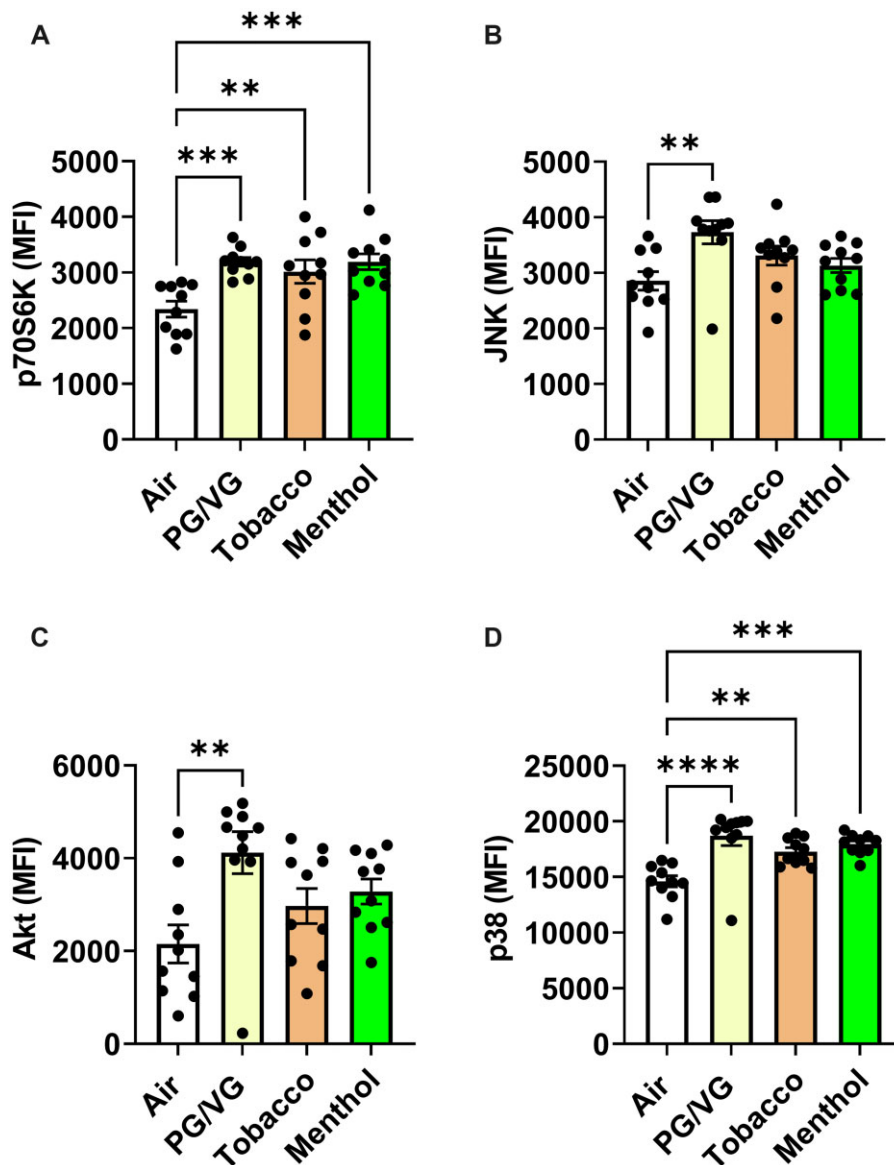
Figure 8. Exposure to PG/VG, menthol, and tobacco flavors in C57BL/6J mouse lung tissue induced PI3K-Akt-mTOR pathway signaling. C57BL/6J male and female mice were exposed to PG/VG, menthol, menthol 6 mg nicotine, tobacco, and tobacco 6 mg nicotine 2 h/day for three consecutive days in SCIREQ whole-body exposure chamber. Mice were euthanized ~24 h postexposure and mouse lung tissues were homogenized and measured cell signaling pathway markers, A, P70S6K; B, JNK; C, Akt; and D, p38 by measuring net median florescence intensity (MFI) normalized to total protein. Data shown as mean ± SEM. $^*p < .05$, $^{**}p < .01$, and $^{***}p < .001$ versus respective air group per strain (1-way ANOVA) ($N = 6$–10 per group).

research (Linke *et al.*, 2017). The observed increase in p38 protein levels suggests aerosol exposure-induced inflammation, cell cycle, cell differentiation, and tumorigenesis by p38-MAP kinase pathway(Zarubin and Han, 2005).

We used Nanostring technology gene expression analyses to elucidate inflammatory and metabolic changes in aerosol-exposed mice. By assessing genes that are significantly altered (upregulated or downregulated) in DNA damage, cellular metabolism, and inflammation, causally networking responses were observed. These data suggested that the immunosuppressive effects maybe correlated to immunometabolism. Our gene expression analysis corroborated PI3K-mTOR mediated signaling responsible for mitochondrial function, metabolism, and immune response regulation, as we observed significant changes in Rps6kb1 serine/threonine kinase of mTOR and PI3K isoforms.

Further, gene expression analysis also showed Arginase-1 alterations, specifically by menthol flavor exposure. Recent studies have shown arginase 1,2 involvement in effector T-cell mediator immunity (O'Neill *et al.*, 2016). Arginine plays a critical distinction between inflammatory and tolerant cell phenotypes via nitic oxide synthase pathway, consistent with the immunoregulatory effects we observed post aerosol exposure. Extracellular vesicles (EVs) carrying Arg have also been found to cause T-cell immunity in antitumor immune responses (Czystowska-Kuzmicz *et al.*, 2019; Singer and Chandel, 2019; Sosnowska *et al.*, 2019). This is consistent with our gene expression changes where anti-tumorigenic and metastatic activity was targeted, eg, ldh3a, Zfp869, and Ash1l. This corroborates our data from the treatment of MLE epithelial cells with isolated EVs from tobacco flavor-exposed mice, which showed significantly altered OCR and ECAR
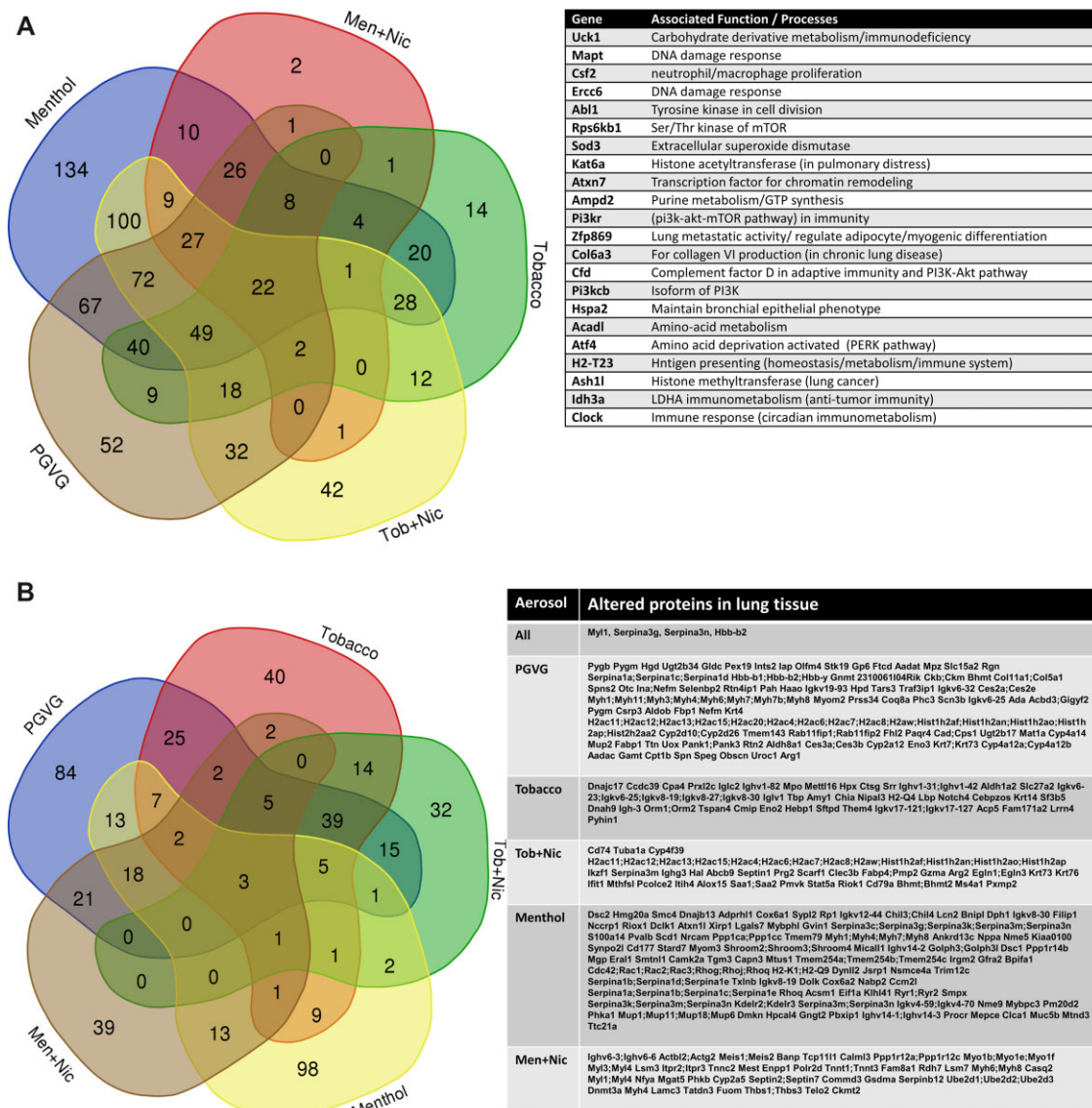
Gene	Associated Function / Processes
Uck1	Carbohydrate derivative metabolism/immunodeficiency
Mapt	DNA damage response
Csf2	neutrophil/macrophage proliferation
Ercc6	DNA damage response
Abl1	Tyrosine kinase in cell division
Rps6kb1	Ser/Thr kinase of mTOR
Sod3	Extracellular superoxide dismutase
Kat6a	Histone acetyltransferase (in pulmonary distress)
Atxn7	Transcription factor for chromatin remodeling
Ampd2	Purine metabolism/GTP synthesis
Pi3kr	(pi3k-akt-mTOR pathway) in immunity
Zfp869	Lung metastatic activity/ regulate adipocyte/myogenic differentiation
Col6a3	For collagen VI production (in chronic lung disease)
Cfd	Complement factor D in adaptive immunity and PI3K-Akt pathway
Pi3kcb	Isoform of PI3K
Hspa2	Maintain bronchial epithelial phenotype
Acadl	Amino-acid metabolism
Atf4	Amino acid deprivation activated (PERK pathway)
H2-T23	Hntigen presenting (homeostasis/metabolism/immune system)
Ash1l	Histone methyltransferase (lung cancer)
Idh3a	LDHA immunometabolism (anti-tumor immunity)
Clock	Immune response (circadian immunometabolism)

Aerosol	Altered proteins in lung tissue
All	Myl1, Serpina3g, Serpina3n, Hbb-b2
PGVG	Pygb Pygm Hgd Ugt2b34 Gldc Pex19 Ints2 Iap Olfm4 Stk19 Gp6 Ftcd Aadat Mpz Slc15a2 Rgn Serpina1a;Serpina1c;Serpina1d Hbb-b1;Hbb-b2;Hbb-y Gnmt 2310061I04Rik Ckb;Ckm Bhmt Col11a1;Col5a1 Spns2 Otc Ina;Nefm Selenbp2 Rtn4ip1 Pah Haao Igkv19-93 Hpd Tars3 Traf3ip1 Igkv6-32 Ces2a;Ces2e Myh1;Myh1;Myh3;Myh4;Myh6;Myh7;Myh7b;Myh8 Myom2 Prss34 Coq8a Phc3 Scn3b Igkv6-25 Ada Acbd3;Gigyf2 Pygm Csrp3 Aldob Fbp1 Nefm Krt4 H2ac11;H2ac12;H2ac13;H2ac15;H2ac20;H2ac4;H2ac6;H2ac7;H2ac8;H2aw;Hist1h2af;Hist1h2an;Hist1h2ao;Hist1h 2ap;Hist2h2aa2 Cyp2d10;Cyp2d26 Tmem143 Rab11flip1;Rab11fip2 Fhl2 Paqr4 Cad;Cps1 Ugt2b17 Mat1a Cyp4a14 Mup2 Fabp1 Ttn Uox Pank1;Pank3 Rtn2 Aldh8a1 Ces3a;Ces3b Cyp2a12 Eno3 Krt7;Krt73 Cyp4a12a;Cyp4a12b Aadac Gamt Cpt1b Spn Speg Obscn Uroc1 Arg1
Tobacco	Dnajc17 Ccdc39 Cpa4 Prxl2c Iglc2 Ighv1-82 Mpo Mettl16 Hpx Ctsg Srr Ighv1-31;Ighv1-42 Aldh1a2 Slc27a2 Igkv6-23;Igkv8-21;Igkv8-19;Igkv8-27;Igkv8-30 Iglv1 Tbp Amy1 Chia Nipal3 H2-Q4 Lbp Notch4 Cebpzos Krt14 Sf3b5 Dnah9 Igh-3 Orm1;Orm2 Tspan4 Cmip Eno2 Hebp1 Sftpd Them4 Igkv17-121;Igkv17-127 Acp5 Fam171a2 Lrrn4 Pyhin1
Tob+Nic	Cd74 Tuba1a Cyp4f39 H2ac11;H2ac12;H2ac13;H2ac15;H2ac4;H2ac6;H2ac7;H2ac8;H2aw;Hist1h2af;Hist1h2an;Hist1h2ao;Hist1h2ap Ikzf1 Serpina3m Ighg3 Hal Abcb9 Septin1 Prg2 Scarf1 Clec3b Fabp4;Pmp2 Gzma Arg2 Eglin1;Egln3 Krt73 Krt76 Ifit1 Mthfsl Pcolce2 Itih4 Alox15 Saa1;Saa2 Pmvk Stat5a Riok1 Cd79a Bhmt;Bhmt2 Ms4a1 Pxmp2
Menthol	Dsc2 Hmg20a Smc4 Dnajb13 Adprhl1 Cox6a1 Sypl2 Rp1 Igkv12-44 Chil3;Chil4 Lcn2 Bnipl Dph1 Igkv8-30 Filip1 Nccrp1 Riox1 Dclk1 Atxn1l Xirp1 Lgals7 Mybphl Gvin1 Serpina3c;Serpina3g;Serpina3k;Serpina3m;Serpina3n S100a14 Pvalb Scd1 Nrcam Ppp1ca;Ppp1cc Tmem79 Myh1;Myh4;Myh7;Myh8 Ankrd13c Nppa Nme5 Kiaa0100 Synpo2l Cd177 Stard7 Myom3 Shroom2;Shroom3;Shroom4 Micall1 Ighv14-2 Golph3;Golph3l Dsc1 Ppp1r14b Mgp Eral1 Smtnl1 Camk2a Tgm3 Capn3 Mtus1 Tmem254a;Tmem254b;Tmem254c Irgm2 Gfra2 Bpifa1 Cdc42;Rac1;Rac2;Rac3;Rhog;Rhoj;Rhoq H2-K1;H2-Q9 Dynll2 Jsrp1 Nsmce4a Trim12c Serpina1b;Serpina1d;Serpina1e Txlnb Igkv8-19 Dolk Cox6a2 Nabp2 Ccm2l Serpina1a;Serpina1b;Serpina1c;Serpina1e Rhoq Acsm1 Eif1a Klhl41 Ryr1;Ryr2 Smpx Serpina3k;Serpina3m;Serpina3n Kdelr2;Kdelr3 Serpina3m;Serpina3n Igkv4-59;Igkv4-70 Nme9 Mybpc3 Pm20d2 Phka1 Mup1;Mup11;Mup18;Mup6 Dmkn Hpcal4 Gngt2 Pbxip1 Ighv14-1;Ighv14-3 Procr Mepce Clca1 Muc5b Mtnd3 Ttc21a
Men+Nic	Ighv6-3;Ighv6-6 Actbl2;Actg2 Meis1;Meis2 Banp Tcp11l1 Calml3 Ppp1r12a;Ppp1r12c Myo1b;Myo1e;Myo1f Myl3;Myl4 Lsm3 Itpr2;Itpr3 Tnnc2 Mest Enpp1 Polr2d Tnnt1;Tnnt3 Fam8a1 Rdh7 Lsm7 Myh6;Myh8 Casq2 Myl1;Myl4 Nfya Mgat5 Phkb Cyp2a5 Septin2;Septin7 Commd3 Gsdma Serpinb12 Ube2d1;Ube2d2;Ube2d3 Dnmt3a Myh4 Lamc3 Tatdn3 Fuom Thbs1;Thbs3 Telo2 Ckmt2

Figure 9. A, Inflammatory and Metabolic gene expression alterations by acute exposure to PG/VG, menthol, menthol with nicotine, tobacco, tobacco with nicotine aerosols. C57BL/6J male and female mice were exposed to three days (2 h/day) air, PG/VG, menthol, menthol + nicotine, tobacco, and tobacco + nicotine aerosols. RNA isolated from lungs were hybridized with Nanostring codesets and the inflammatory and metabolic gene alterations were determined. Genes that ±1.5-fold change altered significantly compared to the Air group were compared. $p < .05$, 1-way ANOVA, N = 6 per group. B, Protein alterations by acute exposure to PG/VG, menthol, menthol with nicotine, tobacco, tobacco with nicotine aerosols. C57BL/6J male and female mice were exposed to three days (2h/day) air, PG/VG, menthol, menthol + nicotine, tobacco, and tobacco flavor + nicotine aerosols. Protein changes were determined by proteomics analysis and presented in a Venn diagram. Proteins significantly altered by 1.5-fold are listed ($p < .05$ vs air group), N = 3 per group.

compared to the air group, suggesting mitochondrial dysfunction and metabolic dysregulation.

Curated proteomics data from each exposure further solidified changes in protein associated with DNA damage, metabolic changes, and immune cell signaling. All aerosol exposures induced significant upregulation of serpinA3. SerpinA3/Antichymotrypsin has been shown to play a role in the inhibition of proteolytic enzymes as well as modulate oncogenic processes by negatively regulating PI3K-Akt-mTOR pathway (Herrero-Sánchez et al., 2016). Further, serpin3a is associated with extracellular matrix remodeling as well as mutations that have been associated with COPD. Aerosol exposures also significantly downregulated Myl protein levels (up to $\log_2$ 8-fold change). Allergic inflammation-induced pulmonary vascular remodeling by OVA

challenge has been shown to downregulate these muscle proteins significantly (Fan et al., 2015).

Overall, the comparative toxicological analysis of brands A and B containing PG/VG, menthol, menthol 6 mg nicotine, tobacco, and tobacco 6 mg nicotine showed differential immune cell influx in BALF, allergic inflammation, and metabolic reprograming in acute exposure with more immunosuppressive effects by menthol. Flavor interactions with nicotine altered these responses. Potential pathways of allergic inflammation include PI3K-Akt-mTOR mediated immunometabolism. More immunosuppressive effects were observed with menthol flavor from both brands A and B. Though tobacco flavor caused more significantly altered cytokines in C57BL/6J compared to BALB/cJ mice, this strain still showed differential responses in inflammatory
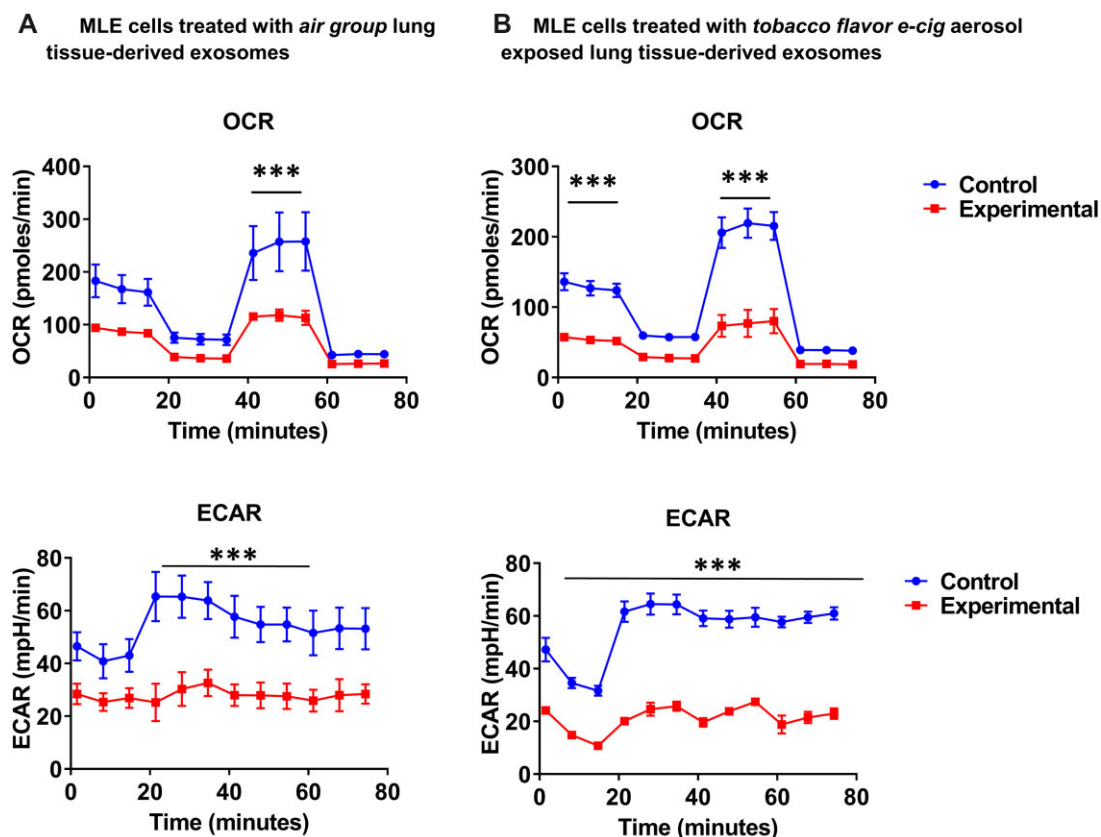
Figure 10. Mitochondrial respiration is affected by extracellular vesicles derived from the lungs of mice exposed to brand B tobacco flavor. C57BL/6J male and female mice were exposed air and tobacco-flavored e-cig aerosols 2 h/day for three consecutive days in SCIREQ whole-body exposure chamber. Mice were euthanized ~24 h postexposure and exosomes were isolated from the lung tissue. MLE15 cells were grown in Seahorse plates and treated with isolated exosomes. Twenty-four hours later, Sea horse mitostress assay was run and oxygen consumption rate (OCR) extracellular acidification rate (ECAR) parameters were acquired, and normalized by total cells. A, MLE cells treated with air group extracellular vesicles (EVs) and B, MLE cells treated with tobacco flavor exposed EVs. *t*-test, ***$p < .001$ versus control, $N = 3$.

mediators and cell counts, suggesting immunoregulatory effects and perhaps is not as susceptible to tobacco flavor constituents. Further, RANTES was identified as a unique player for both tobacco and menthol flavor exposure-induced inflammatory response. Though we did not segregate our data into sex-dependent differences, for specific parameters, we observed more susceptibility in assessed parameters in 1 sex over the other. However, as the differences were statistically not significant due to sample size, sex-specific differences were not a primary focus of this study. The data suggest that T cells were possibly undergoing metabolic reprograming, thus resulting in the suppressed immune response. Our data suggest that chronic exposure to these aerosols may cause lung pathogenesis, including disease susceptibility, reduced bacterial clearance, and potential tumorigenesis.

In conclusion, two brands of the same flavor can cause a differential inflammatory response, genotoxicity, and immunometabolic changes due to flavoring chemical constituents present in the flavored e-liquids and their secondary products in the aerosol. This is likely due to manufacturers utilizing different flavoring chemical compositions containing different constituents, which impart flavor profiles and the purity of ingredients, eg, humectants, nicotine, and solvents. For example, we found high levels of ethanol in the e-liquid aerosols, similar to other studies showing levels of up to 206 mg/ml ethanol in e-liquids (Poklis et al., 2017). Despite our initial hypothesis, by and large, both strains showed similar immunoregulatory responses, but C57BL/

6J showed more significant changes in this 3-day acute exposure model. Chronic exposures are needed to assess strain-dependent differences. The potential mechanism of immune-inflammatory responses is associated with the activation of TRPA1 and PAI-1. As demonstrated by significant adverse responses, Brand A is currently not premarket authorization approved. Our study emphasizes the need to characterize the chemicals in flavored e-liquids and ENDS and perform appropriate toxicological testing in vitro and in vivo to provide insights into regulating e-cig liquids.

Limitations of the current study and future directions

As e-cig aerosols are complex mixtures that depend on many factors, such as temperature, humidity, and airflow, it was challenging to conduct acute toxicity estimates for the mixture. Further, we intend to conduct repeat-dose studies (28–90 days) using menthol (and cooling) and tobacco-flavored aerosols and measure lung mechanics parameters with whole-body plethysmography, pulse oximetry, body weight, micronuclei assessment as nonlethal toxicity parameters and indices. Further, in our next studies, we plan to identify additive and synergistic effects of common chemical constituents present in the liquid and the aerosol. Determining the most toxic chemicals and ascertaining their toxicological parameters and indices would be useful in predictive toxicity assessments.

While we kept an on-average record of the particle size distribution (250 mg/m^3, PM 1.0), conducting real-time particle size
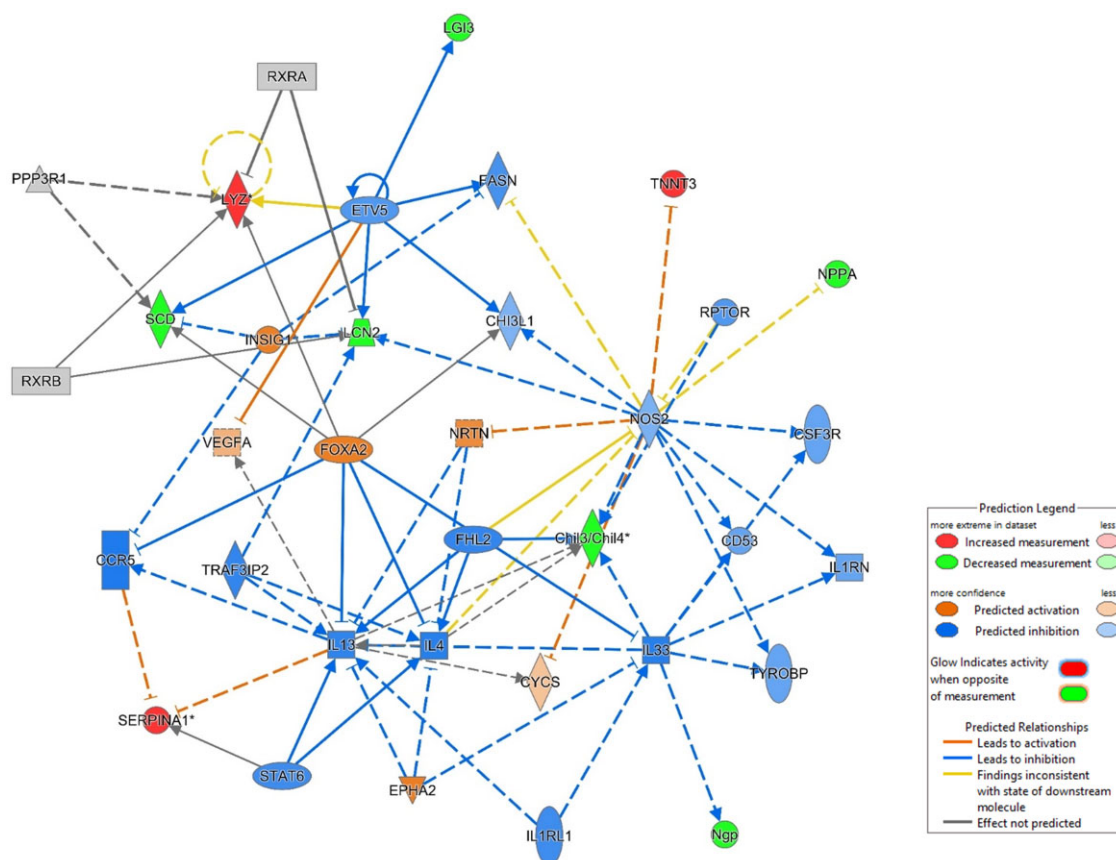
Figure 11. Potential pathways of immunometabolic and allergic inflammatory response via PI3K-Akt-mTOR. C57BL/6J male and female representative canonical pathway of menthol e-cig flavor exposure-induced lung response by ingenuity pathway analysis of proteomics data demonstrating inhibition of inflammatory pathways and upregulating immunoregulatory pathways.

and distribution during exposures was challenging. Hence, in future studies, we intend to integrate a scanning mobility particle sizer for real-time particle size distribution measurements within the exposure chamber.

Another limitation of the study would be inconsistency or incorrect labeling of ingredients on the bottles by manufacturers, such as the nicotine concentration, as we determined marginal levels of nicotine in zero mg flavor liquids, which further emphasizes the need for the proper regulation of e-liquid constituents and enforcements of policies.

Supplementary data

Supplementary data are available at *Toxicological Sciences* online.

Declaration of conflicting interests

The authors declare that the research was conducted in the absence of any commercial or financial relationships that could be construed as a potential conflict of interest, and no potential conflicts of interest with respect to the authorship, and/or publication of this article.

Author contributions

T.M. and I.R. conceived and designed the experiments. T.M. performed the experiments, analyzed data, and wrote the article. I.R. edited the article.

Data availability

We declare that we have provided all the data, but the primary data will be available upon request.

References

Alam, R., York, J., Boyars, M., Stafford, S., Grant, J., A., Lee, J., Forsythe, P., Sim, T., and Ida, N. (1996). Increased MCP-1, RANTES, and MIP-1alpha in bronchoalveolar lavage fluid of allergic asthmatic patients. *Am. J. Respir. Crit. Care Med.* **153**, 1398–1404.

Alexander, L. E. C., Bellinghausen, A. L., and Eakin, M. N. (2020). What are the mechanisms underlying vaping-induced lung injury? *J. Clin. Invest.* **130**, 2754–2756.

Ali, F. R. M., Seaman, E. L., Diaz, M. C., Ajose, J., and King, B. A. (2022). Trends in unit sales of cooling flavoured e-cigarettes, USA, 2017-2021. *Tob. Control.* 1052–1056. doi:10.1136/tc-2022-057395.

Birrell, M. A., Belvisi, M. G., Grace, M., Sadofsky, L., Faruqi, S., Hele, D. J., Maher, S., A., Freund-Michel, V., and Morice, A. H. (2009). TRPA1 agonists evoke coughing in guinea pig and human volunteers. *Am. J. Respir. Crit. Care Med.* **180**, 1042–1047.

Bitzer, Z., T., Goel, R., Reilly, S. M., Foulds, J., Muscat, J., Elias, R. J., and Richie, J. P., Jr (2018). Effects of solvent and temperature on free radical formation in electronic cigarette aerosols. *Chem. Res. Toxicol.* **31**, 4–12.

Brumpton, B. M., Camargo, C. A., Jr, Romundstad, P. R., Langhammer, A., Chen, Y., and Mai, X. M. (2013). Metabolic syndrome and incidence of asthma in adults: the HUNT study. *Eur. Respir. J.* **42**, 1495–1502.

Caceres, A. I., Brackmann, M., Elia, M. D., Bessac, B. F., del Camino, D., D'Amours, M., Witek, J. S., Fanger, C. M., Chong, J. A., Hayward, N. J., et al (2009). A sensory neuronal ion channel essential for airway inflammation and hyperreactivity in asthma. *Proc. Natl. Acad. Sci. U S A* **106**, 9099–9104.

Chou, W. C., Rampanelli, E., Li, X., and Ting, J. P. (2022). Impact of intracellular innate immune receptors on immunometabolism. *Cell. Mol. Immunol.* **19**, 337–351.

Crotty Alexander, L. E., Drummond, C. A., Hepokoski, M., Mathew, D., Moshensky, A., Willeford, A., Das, S., Singh, P., Yong, Z., Lee, J. H., et al (2018). Chronic inhalation of e-cigarette vapor containing nicotine disrupts airway barrier function and induces systemic inflammation and multiorgan fibrosis in mice. *Am. J. Physiol. Regul. Integr. Comp. Physiol.* **314**, R834–R847.

Czystowska-Kuzmicz, M., Sosnowska, A., Nowis, D., Ramji, K., Szajnik, M., Chlebowska-Tuz, J., Wolinska, E., Gaj, P., Grazul, M., Pilch, Z., et al (2019). Small extracellular vesicles containing arginase-1 suppress T-cell responses and promote tumor growth in ovarian carcinoma. *Nat. Commun.* **10**, 3000.

Deben, C., Deschoolmeester, V., Lardon, F., Rolfo, C., and Pauwels, P. (2016). TP53 and MDM2 genetic alterations in non-small cell lung cancer: evaluating their prognostic and predictive value. *Crit. Rev. Oncol. Hematol.* **99**, 63–73.

Deben, C., Wouters, A., Op de Beeck, K., van Den Bossche, J., Jacobs, J., Zwaenepoel, K., Peeters, M., Van Meerbeeck, J., Lardon, F., Rolfo, C., et al (2015). The MDM2-inhibitor Nutlin-3 synergizes with cisplatin to induce p53 dependent tumor cell apoptosis in non-small cell lung cancer. *Oncotarget* **6**, 22666–22679.

Diaz, M. C., Donovan, E. M., Schillo, B. A., and Vallone, D. (2021). Menthol e-cigarette sales rise following 2020 FDA guidance. *Tob. Control.* **30**, 700–703.

Fan, C., Meuchel, L. W., Su, Q., Angelini, D. J., Zhang, A., Cheadle, C., Kolosova, I., Makarevich, O. D., Yamaji-Kegan, K., Rothenberg, M. E., et al (2015). Resistin-like molecule alpha in allergen-induced pulmonary vascular remodeling. *Am. J. Respir. Cell Mol. Biol.* **53**, 303–313.

Finucane, O. M., Sugrue, J., Rubio-Araiz, A., Guillot-Sestier, M. V., and Lynch, M. A. (2019). The NLRP3 inflammasome modulates glycolysis by increasing PFKFB3 in an IL-1beta-dependent manner in macrophages. *Sci. Rep.* **9**, 4034.

Galderisi, A., Ferraro, V. A., Caserotti, M., Quareni, L., Perilongo, G., and Baraldi, E. (2020). Protecting youth from the vaping epidemic. *Pediatr. Allergy Immunol.* **31** Suppl 26, 66–68.

Gotts, J. E., Jordt, S. E., McConnell, R., and Tarran, R. (2019). What are the respiratory effects of e-cigarettes? *Bmj* **366**, l5275.

Hajna, Z., Cseko, K., Kemeny, A., Kereskai, L., Kiss, T., Perkecz, A., Szitter, I., Kocsis, B., Pinter, E., and Helyes, Z. (2020). Complex regulatory role of the TRPA1 receptor in acute and chronic airway inflammation mouse models. *Int J Mol Sci* **21**, 4109.

Hamberger, E. S., and Halpern-Felsher, B. (2020). Vaping in adolescents: epidemiology and respiratory harm. *Curr. Opin. Pediatr.* **32**, 378–383.

Han, S., Jerome, J. A., Gregory, A. D., and Mallampalli, R. K. (2017). Cigarette smoke destabilizes NLRP3 protein by promoting its ubiquitination. *Respir. Res.* **18**, 2.

Hancock, L. A., Hennessy, C. E., Solomon, G. M., Dobrinskikh, E., Estrella, A., Hara, N., Hill, D. B., Kissner, W. J., Markovetz, M. R., Grove Villalon, D. E., et al (2018). Muc5b overexpression causes mucociliary dysfunction and enhances lung fibrosis in mice. *Nat. Commun.* **9**, 5363.

Herrero-Sánchez, M. C., Rodríguez-Serrano, C., Almeida, J., San-Segundo, L., Inogés, S., Santos-Briz, Á., García-Briñón, J., SanMiguel, J. F., Del Cañizo, C., and Blanco, B. (2016). Effect of mTORC1/mTORC2 inhibition on T cell function: potential role in graft-versus-host disease control. *Br. J. Haematol.* **173**, 754–768.

Hickman, E., Herrera, C. A., and Jaspers, I. (2019). Common E-cigarette flavoring chemicals impair neutrophil phagocytosis and oxidative burst. *Chem. Res. Toxicol.* **32**, 982–985.

Hua, M., Omaiye, E. E., Luo, W., McWhirter, K. J., Pankow, J. F., and Talbot, P. (2019). Identification of cytotoxic flavor chemicals in top-selling electronic cigarette refill fluids. *Sci. Rep.* **9**, 2782.

Jabba, S. V., Diaz, A. N., Erythropel, H. C., Zimmerman, J. B., and Jordt, S. E. (2020). Chemical adducts of reactive flavor aldehydes formed in E-cigarette liquids are cytotoxic and inhibit mitochondrial function in respiratory epithelial cells. *Nicotine Tob. Res.* **22**, S25–S34.

Kaur, G., Muthumalage, T., and Rahman, I. (2018). Mechanisms of toxicity and biomarkers of flavoring and flavor enhancing chemicals in emerging tobacco and non-tobacco products. *Toxicol. Lett.* **288**, 143–155.

Khlystov, A., and Samburova, V. (2016). Flavoring compounds dominate toxic aldehyde production during e-cigarette vaping. *Environ. Sci. Technol.* **50**, 13080–13085.

King, B. A., and Kingma, P. S. (2011). Surfactant protein D deficiency increases lung injury during endotoxemia. *Am. J. Respir. Cell Mol. Biol.* **44**, 709–715.

Koivisto, A. P., Belvisi, M. G., Gaudet, R., and Szallasi, A. (2022). Advances in TRP channel drug discovery: from target validation to clinical studies. *Nat. Rev. Drug Discov.* **21**, 41–59.

Koya, T., Takeda, K., Kodama, T., Miyahara, N., Matsubara, S., Balhorn, A., Joetham, A., Dakhama, A., and Gelfand, E. W. (2006). RANTES (CCL5) regulates airway responsiveness after repeated allergen challenge. *Am. J. Respir. Cell Mol. Biol.* **35**, 147–154.

Krämer, A., Green, J., Pollard, J., Jr, and Tugendreich, S. (2014). Causal analysis approaches in Ingenuity Pathway Analysis. *Bioinformatics* **30**, 523–530.

Kuo, L. J., and Yang, L. X. (2008). Gamma-H2AX – a novel biomarker for DNA double-strand breaks. *In Vivo* **22**, 305–309.

Lamb, T., Muthumalage, T., Meehan-Atrash, J., and Rahman, I. (2022). Nose-only exposure to cherry- and tobacco-flavored e-cigarettes induced lung inflammation in mice in a sex-dependent manner. *Toxics* **10**, 471.

Lamb, T., Muthumalage, T., and Rahman, I. (2020). Pod-based menthol and tobacco flavored e-cigarettes cause mitochondrial dysfunction in lung epithelial cells. *Toxicol. Lett.* **333**, 303–311.

Lei, W., Lerner, C., Sundar, I. K., and Rahman, I. (2017). Myofibroblast differentiation and its functional properties are inhibited by nicotine and e-cigarette via mitochondrial OXPHOS complex III. *Sci. Rep.* **7**, 43213.

Lerner, C. A., Sundar, I. K., Watson, R. M., Elder, A., Jones, R., Done, D., Kurtzman, R., Ossip, D. J., Robinson, R., McIntosh, S., et al (2015). Environmental health hazards of e-cigarettes and their components: oxidants and copper in e-cigarette aerosols. *Environ. Pollut.* **198**, 100–107.

Levy, D. T., Yuan, Z., Li, Y., Mays, D., and Sanchez-Romero, L. M. (2019). An examination of the variation in estimates of e-cigarette prevalence among U.S. adults. *Int J Environ Res Public Health* **16**, 3164.

Li, N., Mirzakhani, H., Kiefer, A., Koelle, J., Vuorinen, T., Rauh, M., Yang, Z., Krammer, S., Xepapadaki, P., Lewandowska-Polak, A., et al 2021a). Regulated on Activation, Normal T cell Expressed and Secreted (RANTES) drives the resolution of allergic asthma. *iScience* **24**, 103163.

Li, Y., Burns, A. E., Tran, L. N., Abellar, K. A., Poindexter, M., Li, X., Madl, A. K., Pinkerton, K. E., and Nguyen, T. B. (2021b). Impact of e-liquid composition, coil temperature, and puff topography on the aerosol chemistry of electronic cigarettes. *Chem. Res. Toxicol.* **34**, 1640–1654.

Linke, M., Fritsch, S. D., Sukhbaatar, N., Hengstschlager, M., and Weichhart, T. (2017). mTORC1 and mTORC2 as regulators of cell metabolism in immunity. *FEBS Lett.* **591**, 3089–3103.

Lloyd, C. M., and Murdoch, J. R. (2010). Tolerizing allergic responses in the lung. *Mucosal Immunol.* **3**, 334–344.

Lucas, J. H., Muthumalage, T., Wang, Q., Friedman, M. R., Friedman, A. E., and Rahman, I. (2020). E-liquid containing a mixture of coconut, vanilla, and cookie flavors causes cellular senescence and dysregulated repair in pulmonary fibroblasts: implications on premature aging. *Front. Physiol.* **11**, 924.

Marechal, A., and Zou, L. (2013). DNA damage sensing by the ATM and ATR kinases. *Cold Spring Harb Perspect Biol* **5**, a012716.

Martin, E. M., Clapp, P. W., Rebuli, M. E., Pawlak, E. A., Glista-Baker, E., Benowitz, N. L., Fry, R. C., and Jaspers, I. (2016). E-cigarette use results in suppression of immune and inflammatory-response genes in nasal epithelial cells similar to cigarette smoke. *Am. J. Physiol. Lung Cell. Mol. Physiol.* **311**, L135–44.

Mayer, M., Reyes-Guzman, C., Grana, R., Choi, K., and Freedman, N. D. (2020). Demographic characteristics, cigarette smoking, and e-cigarette use among US adults. *JAMA Netw. Open.* **3**, e2020694.

Meyer, K. C., Raghu, G., Baughman, R. P., Brown, K. K., Costabel, U., du Bois, R. M., Drent, M., Haslam, P. L., Kim, D. S., Nagai, S., et al; American Thoracic Society Committee on BAL in Interstitial Lung Disease. (2012). An official American Thoracic Society clinical practice guideline: the clinical utility of bronchoalveolar lavage cellular analysis in interstitial lung disease. *Am J Respir Crit Care Med* **185**, 1004–1014.

Miech, R., Leventhal, A., Johnston, L., O'Malley, P. M., Patrick, M. E., and Barrington-Trimis, J. (2021). Trends in use and perceptions of nicotine vaping among US youth from 2017 to 2020. *JAMA Pediatr.* **175**, 185–190.

Moilanen, L. J., Laavola, M., Kukkonen, M., Korhonen, R., Leppanen, T., Hogestatt, E. D., Zygmunt, P. M., Nieminen, R. M., and Moilanen, E. (2012). TRPA1 contributes to the acute inflammatory response and mediates carrageenan-induced paw edema in the mouse. *Sci. Rep.* **2**, 380.

Muthumalage, T., Friedman, M. R., McGraw, M. D., Ginsberg, G., Friedman, A. E., and Rahman, I. (2020). Chemical constituents involved in e-cigarette, or vaping product use-associated lung injury (EVALI). *Toxics* **8**, 25.

Muthumalage, T., Lamb, T., Friedman, M. R., and Rahman, I. (2019). E-cigarette flavored pods induce inflammation, epithelial barrier dysfunction, and DNA damage in lung epithelial cells and monocytes. *Sci. Rep.* **9**, 19035.

Muthumalage, T., Prinz, M., Ansah, K. O., Gerloff, J., Sundar, I. K., and Rahman, I. (2017). Inflammatory and oxidative responses

induced by exposure to commonly used e-cigarette flavoring chemicals and flavored e-liquids without nicotine. *Front. Physiol.* **8**, 1130.

Neveu, W. A., Allard, J. L., Raymond, D. M., Bourassa, L. M., Burns, S. M., Bunn, J. Y., Irvin, C. G., Kaminsky, D. A., and Rincon, M. (2010). Elevation of IL-6 in the allergic asthmatic airway is independent of inflammation but associates with loss of central airway function. *Respir. Res.* **11**, 28.

O'Neill, L. (2017). Immunometabolism and the land of milk and honey. *Nat. Rev. Immunol.* **17**, 217.

O'Neill, L. A., Kishton, R. J., and Rathmell, J. (2016). A guide to immunometabolism for immunologists. *Nat. Rev. Immunol.* **16**, 553–565.

Omaiye, E. E., McWhirter, K. J., Luo, W., Tierney, P. A., Pankow, J. F., and Talbot, P. (2019). High concentrations of flavor chemicals are present in electronic cigarette refill fluids. *Sci. Rep.* **9**, 2468.

Palsson-McDermott, E. M., and O'Neill, L. A. J. (2020). Targeting immunometabolism as an anti-inflammatory strategy. *Cell Res.* **30**, 300–314.

Poklis, J. L., Wolf, C. E., 2nd., and Peace, M. R. (2017). Ethanol concentration in 56 refillable electronic cigarettes liquid formulations determined by headspace gas chromatography with flame ionization detector (HS-GC-FID). *Drug Test. Anal.* **9**, 1637–1640.

Prabhakaran, P., Ware, L. B., White, K. E., Cross, M. T., Matthay, M. A., and Olman, M. A. (2003). Elevated levels of plasminogen activator inhibitor-1 in pulmonary edema fluid are associated with mortality in acute lung injury. *Am. J. Physiol. Lung Cell. Mol. Physiol.* **285**, L20–8.

Rincon, M., and Irvin, C. G. (2012). Role of IL-6 in asthma and other inflammatory pulmonary diseases. *Int. J. Biol. Sci.* **8**, 1281–1290.

Sabatini, D. M. (2017). Twenty-five years of mTOR: uncovering the link from nutrients to growth. *Proc. Natl. Acad. Sci. U S A* **114**, 11818–11825.

Sinclair, C., Bommakanti, G., Gardinassi, L., Loebbermann, J., Johnson, M. J., Hakimpour, P., Hagan, T., Benitez, L., Todor, A., Machiah, D., et al (2017). mTOR regulates metabolic adaptation of APCs in the lung and controls the outcome of allergic inflammation. *Science* **357**, 1014–1021.

Singer, B. D., and Chandel, N. S. (2019). Immunometabolism of prorepair cells. *J. Clin. Invest.* **129**, 2597–2607.

Sosnowska, A., Czystowska-Kuzmicz, M., and Golab, J. (2019). Extracellular vesicles released by ovarian carcinoma contain arginase 1 that mitigates antitumor immune response. *Oncoimmunology* **8**, e1655370.

Szafran, B. N., Pinkston, R., Perveen, Z., Ross, M. K., Morgan, T., Paulsen, D. B., Penn, A. L., Kaplan, B. L. F., and Noel, A. (2020). Electronic-cigarette vehicles and flavoring affect lung function and immune responses in a murine model. *Int J Mol Sci* **21**, 6022.

Wang, Q., Sundar, I. K., Li, D., Lucas, J. H., Muthumalage, T., McDonough, S. R., and Rahman, I. (2020). E-cigarette-induced pulmonary inflammation and dysregulated repair are mediated by nAChR alpha7 receptor: role of nAChR alpha7 in SARS-CoV-2 Covid-19 ACE2 receptor regulation. *Respir. Res.* **21**, 154.

Wang, Q., and Wu, H. (2018). T cells in adipose tissue: critical players in immunometabolism. *Front. Immunol.* **9**, 2509.

Ward, I. M., and Chen, J. (2001). Histone H2AX is phosphorylated in an ATR-dependent manner in response to replicational stress. *J. Biol. Chem.* **276**, 47759–47762.

Zarubin, T., and Han, J. (2005). Activation and signaling of the p38 MAP kinase pathway. *Cell Res.* **15**, 11–18.

Zidovetzki, R., Chen, P., Fisher, M., Hofman, F. M., and Faraci, F. M. (1999). Nicotine increases plasminogen activator inhibitor-1 production by human brain endothelial cells via protein kinase C-associated pathway. *Stroke* **30**, 651–655.